Relationships between fluvial evolution and karstification related to climatic, tectonic and eustatic forcing in temperate regions

Dominique Harmand, Kathryn Adamson, Gilles Rixhon, Stéphane Jaillet, Benoît Losson, Alain Devos, Gabriel Hez, Marc Calvet, Philippe Audra

Relationships between fluvial evolution and karstification related to climatic, tectonic and eustatic forcing in temperate regions

Dominique Harmand[a], Kathryn Adamson[b], Gilles Rixhon[c], Stéphane Jaillet[d], Benoît Losson[a], Alain Devos[e], Gabriel Hez[d], Marc Calvet[f], Philippe Audra[g]

[a]Laboratoire LOTERR, Université de Lorraine, site Libération, BP 13387, 54015 Nancy, (F). dominique.harmand@univ-lorraine.fr, benoit.losson@univ-lorraine.fr

[b]School of Science and The Environment, Manchester Metropolitan University, M1 5GD Manchester (UK). k.adamson@mmu.ac.uk

[c]University of Cologne Institute for Geography, Albertus-Magnus-Platz 50923 Köln (D). grixhon@uni-koeln.de

[d]Laboratoire EDYTEM, Université de Savoie, CNRS, Pôle Montagne, F - 73376 Le Bourget du Lac (F). Stephane.Jaillet@univ-savoie.fr, gabrielhez@orange.fr

[e]Genenaa, 2 esplanade Roland Garros 51100 REIMS (F). alain.devos@univ-reims.fr

[f]Université de Perpignan-Via Domitia, UMR 7194 HNHP, 66860 Perpignan Cedex (F). calvet@univ-perp.fr

[g]Polytech Nice - Sophia Université de Nice - Sophia Antipolis 930 route des Colles 06903 Sophia-Antipolis (F). audra@unice.fr

Abstract

This paper reviews the diversity of relationships between river evolution and karstogenesis. It also underlines the fundamental role of numerical dating methods (e.g. cosmogenic nuclides) applied to sedimentary sequences in tiered cave passages as they have provided new insights into these complex interactions. Although karst terrain is widespread worldwide, we focus on European karst catchments, where the sedimentary records are especially well preserved. We review the recent dating of fluvial sediments and speleothems, to examine the timing of karstification, incision and deposition in cave levels. The most complete alluvial records occur in tectonically uplifted high mountains where some of the oldest sediment fills date to the Miocene. Evidence indicates that not only uplift, but also climatic conditions and fluvial dynamics (e.g. knickpoint retreat, increased channel flow and/or sediment load, and stream piracies) can play a major role in speleogenesis and geomorphological evolution. In evaporite rocks, speleogenesis is characterized by rapid dissolution and subsidence. In European catchments, gypsum cave development largely occurred during cold climate periods, while

limestone caves formed during warm interglacial or interstadial phases. Our synthesis is used to propose four models of fluvial and karst evolution, and highlight perspectives for further research.

Keys words: karst, speleogenesis, valley incision, aggradation, base level, cave level, phreatic cave, cosmogenic nuclide dating

1. Introduction: links between karst and fluvial systems

1.1. Conditions and processes of karstification

Karst terrain is characterised by underground drainage networks and (sub)surface features such as dolines, poljes, sinkholes, and caves (Palmer, 2007). It is typical of regions of limestone, evaporite and marble bedrock, but also develops in siliceous (sandstones and quartzites) and other metamorphic rocks (Ford & Williams, 1989; Bigot & Audra, 2010). According to Ford and Williams (1989), karst is globally present in all climate domains, but the widest areas of karstified terrain are in the limestone and evaporite regions of Europe and Asia (Figure 1). Karstification is the process of water infiltration and dissolution, mainly through chemical mechanisms, involving the presence of water and carbonic acid. This definition implies strong links between karst and fluvial activity, especially for epigenetic speleogenesis which involves the vertical organization of 'three karstic horizons' (Mangin, 1975; Audra & Palmer, 2013): the infiltration of water at the surface; the flow of water through karstified limestones or evaporites; and the emergence of water from karst conduits at the valley bottom (Ek, 1961; Delannoy, 1997; Audra, 2010, Figure 2A, 2B). Water flow, and resulting sediment transport, along the three 'karstic horizons' (Mangin, 1975) means that subaerial fluvial forms such as terraces, often contain only generalized records of palaeo-base and cave levels. Therefore, the core topic of this contribution focuses on the combined analysis of surface alluvial sequences and subterranean (endokarst) geomorphology and sediment fills, which produces more complete reconstructions of palaeofluvial activity in karst settings.

In karst regions, alluvium is often well-preserved in endokarstic cavities. The most distinctive endokarstic features are the horizontal tubes that form in the saturated zone: syngenetic and paragenetic galleries, the latter of which form upward to the water table (e.g. Ford & Williams, 1989; Quinif, 1989). These features correspond to periods of base level stability in the fluvial system. In contrast, meandering canyons and vadose shafts form in the unsaturated zone, and

may be correlated to incision in the adjacent valleys (Audra & Palmer, 2011). The transition from phreatic to vadose conditions produces keyhole (T-form) features, and the reshaping of previously enlarged passages and narrow and deep underground canyons during river entrenchment phases.

In limestone karst, cave formation occurs due to the dissolution of bedrock by unsaturated water containing carbonic acid (from CO_2) (Palmer, 1991). The maximal denudation rates in the temperate zone occur in the wetter oceanic regions (even in wet subarctic areas), such as in Chilean Patagonia (100 mm/ka, Hobléa *et al.,* 2001) or in the Vercors, French subalpine chains (120-170 mm/ka, Delannoy, 1982), and primarily depend on the amount of precipitation (Palmer, 1991). Under interglacial and interstadial conditions, forest soils are well-developed, and these can be an especially aggressive dissolution agent (Ford & Williams, 1989; Quinif, 2006). White (1988) highlighted the existence of thresholds in the development of cave passages. First, a laminar flow regime produces micro-caves (diameter: 5-10 mm) during an initiation phase of 3-5 ka. Then, turbulent flow can shape 1-3 m conduits within a few thousand years during a phase of enlargement. In high alpine mountains, where high precipitation and acidic forest soils mean that cave development can be especially rapid, wide conduits (from 1 to 10 m) can appear in a few hundred years (Ford & Williams, 1989).

The propagation of groundwater through a karst system is largely determined by its structural framework (Ford & Williams, 1989). In limestone, only planes of penetrable fissures (e.g. bedding planes, stratification joints, faults) have sufficient permeability. In rocks with greater fracturation, permeability is higher due to decreased anisotropy (Bazalgette & Petit, 2005). For example, in folded rocks that have been subjected to tectonic stresses, fissure frequency and therefore permeability, is generally higher (Ford & Williams, 1989). Fissure frequency also increases over time, in relation to solvent water infiltration (Gabrovšek et *al.,* 2014) and rock decompression due to valley entrenchment. These structural controls on subterranean morphology also explain the existence of caves in non karstified areas: opened faults, underground collapse structures, or caves shaped in impervious rocks. For example, the Verna cave (Pyrenees, the biggest cave chamber in France), is mainly situated in Carboniferous sandstone and shales (Gilli, 2010). In general, geomorphological maps of karstified areas show parallel horizontal passages, aligned with the main regional fractures (Losson, 2003) and, sometimes, a gridded cave network of intersecting, fracture-controlled fissures (Palmer, 1991; Audra & Palmer, 2011). However, fluvial geometry can develop independently of structural

103 controls, such as in the Eastern Paris Basin, where rivers are superimposed on the Mesozoic
104 strata (Le Roux & Harmand, 1998, 2003).
105
106 **1.2. Types of cave sedimentary fill**
107
108 Cave deposits are highly variable in their origin and characteristics, and include allochthonous
109 and autochthonous sediments which can be broadly categorized as coarse and fine-grained
110 clastic sediments, and carbonate precipitates. The most common cave formations are the coarse
111 clastic deposits of the entrance facies. In the glaciated parts of Europe and North America much
112 of this clastic material is derived from glacial till and deglacial sediments (Granger *et al.,* 2001).
113 In non–glaciated areas, clastic deposits are the result of bedrock breakdown and decompression
114 close to the valley sides as well as cryoclastic processes at the cave entrance (Campy, 1982).
115 Cryoclastic sediments can include palaeontological and/or archaeological remains, such as in
116 the "Belle-Roche" cave, developed in the Carboniferous limestone of the Amblève valley
117 (Ardenne massif, E. Belgium; Cordy *et al.,* 1993; Rixhon *et al.,* 2014). There, the archaeo-
118 palaeotolongical layers overlie basal Amblève gravels, indicative of a palaeovalley floor
119 position (Rixhon & Demoulin, 2010). The presence of such coarse sediments, deposited by high
120 energy flows, generally indicate a period of enhanced fluvial activity in the cave environment
121 (Ford & Williams, 1989).
122
123 Secondary carbonates are formed by the dissolution of calcium carbonate in the karst bedrock
124 and its reprecipitation, producing features such as tufa, travertine, and speleothems (Couchoud,
125 2008). These precipitates develop in association with prevailing environmental conditions, and
126 reflect changes in water percolation, evaporation and degassing. They can therefore provide
127 valuable records of palaeoclimate, palaeoecology, and palaeogeomorphology – since tufa and
128 travertine cap palaeoland surfaces. Moreover, they can be dated by radiocarbon (^{14}C) and
129 Uranium-series (U-series) methods. Speleothems in particular can provide very high temporal
130 resolution palaeoclimatic data due to their banded nature. Tufa and travertine *(sensu lato)* are
131 more complex, and can form in multiple, superimposed horizons or tiered steps of different
132 ages (Ford & Williams, 1989).
133
134 **1.3. Markers of Pleistocene valleys evolution**
135

Many studies have thoroughly discussed the relationships between karst terrain and catchment sediment flux, incision and aggradation (Benito *et al.,* 1998, 2010; Granger & Palmer, 2001; Jaillet *et al.,* 2004; Mocochain *et al.,* 2009; Audra & Palmer, 2011; Guifang *et al.,* 2011; Calvet *et al.,* 2015; Columbu *et al.,* 2015). During the Pleistocene, karst evolution was conditioned by climatically-driven cycles of river incision and aggradation, operating over 41 ka and 100 ka timescales (Bridgland & Westaway, 2007). In most cases, cave levels formed following entrenchment of rivers into limestone rocks, lowering the piezometric level. Incision into preexisting alluvium and the substratum occurred either during warm–cold (e.g. karst of N France; Antoine, 1994) or cold–warm transitional periods (e.g. British karst; Bridgland & Westaway, 2007; Lewin & Gibbard, 2010). Aggradation occurred chiefly during cold periods, characterised by massive deposition of gravel and sand,. Evidence of other cold climate indicators, such as ice-rafted blocks, ice wedges, and cryoturbation, have also been identified in karst alluvial sequences. River gravels at the valley bottom (e.g. Antoine *et al.,* 2006) or terraces (e.g. Bridgland *et al.,* 2009) are sometimes covered by interglacial or interstadial alluvial silt, soils, peat, and tufa.

Evidence of progressive stacking of alluvial sequences indicates the raising of cave level (Audra & Palmer, 2011), while fill-in-fill terraces imply a succession of lowering and raising of base and caves levels. At the valley scale, Pleistocene uplift generates tiered terraces provided that progressive vertical fluvial incision was accompanied by lateral erosion due to channel migration (Lewin & Gibbard, 2010). In karst areas where only few remnants of strath terraces are preserved along deeply-incised canyons, only infilled caves can be used to precisely reconstruct the evolution of Pleistocene valley entrenchment (Audra *et al.,* 2001).

In karstic fluvial settings, sediment sources, transportation and deposition characteristics vary in accordance with Quaternary environmental changes. On the one hand during glacial and periglacial periods, enhanced sediment mobilization means that clastic sediment can become trapped in caves and karst depressions (Audra *et al.,* 2001; Audra, Ed, 2010; Rixhon *et al.*, 2014; Calvet *et al.,* 2015). In areas covered by ice-sheets, sedimentation ceases. On the other hand, during interstadial, interglacial, and postglacial climates, tufa, travertine, and speleothems generally developed as a result of prolonged valley floor stability (Delannoy, 1997; Frank *et al.,* 2006; Limondin-Lozouet *et al.,* 2006; Couchoud, 2008).

Endokarstic alluvial deposits thus have the potential to offer a valuable record of Quaternary river system evolution. However, fragmentary nature of endokarstic deposits, and their

integration with other sedimentary records over different timescales are two key issues that need to be addressed. Can endokarstic fluvial deposits be reliably integrated with other alluvial records to produce a model of Quaternary valley evolution? Can we combine records from fragmentary time slices into the same landscape evolution model (valley terraces, isolated endokarstic remnants, tiered passages in karst massifs)?

This paper presents a synthesis of recent research in European karst river systems (where appropriate, we also refer to well-studied non-European karst settings), developed within the modern temperate climate zone (Fig.1). It considers multiple spatial scales, from localized cave deposits to regional palaeoenvironmental reconstructions. It also discusses climatic, glacial, tectonic, isostatic, and eustatic forcing on karstogenesis (lowered sea level causes rejuvenation of karst processes, and subsequent raised sea level generates successive cave levels in systems fluvially linked to coastal locations), as well as the increasing application of dating methods on alluvial sediments in karst terrains, such as U-series, terrestrial cosmogenic nuclide (TCN) and ^{14}C. We establish a typology of the relationships between speleogenesis and fluvial incision/aggradation. Finally, we propose four conceptual models of karstic fluvial development based on the reviewed literature.

We examine their Quaternary development which is influenced by periglacial and glacial processes in mountain settings. In glaciated areas, fluvial discharge would have been directly linked to glacier mass balance (see 4.3). In periglacial settings, river flow regime would have been strongly influenced by precipitation and temperature variability.

2. Dating methods in karstic environments

Until the 1980s and 1990s, relative dating techniques (notably palynology and palaeomagnetism) were the primary methods used to estimate the age of fluvial deposits in karst terrain (Ford & Williams, 1989). Several numerical dating methods, such as thermoluminescence (TL, Huxtable and Aitken, 1991), uncalibrated radiocarbon (^{14}C, Bastin & Gewelt, 1986) and Uranium-series (U-series) in caves and river terrace calcrete were also used (Ambert & Ambert, 1995). Advances in numerical dating methods during the last two decades have allowed more robust chronologies to be developed (Couchoud, 2008; Richard *et al.,* 2015; Rixhon *et al.*, 2016). Calibrated radiocarbon ages (cal ^{14}C), optically stimulated luminescence (OSL, e. g. Vernet *et al.,* 2008), and electron spin resonance (ESR, e. g. Moreno

et al., 2012) techniques have become more widely applied. Terrestrial cosmogenic nuclide (TCN) dating of karst environments, especially burial dating, has also greatly enhanced the understanding of complex interactions between karst and fluvial systems (Granger *et al.,* 1997).

2.1. Numerical methods to date tufa, travertine and fluvial calcrete

Secondary carbonates, such as tufa, travertine, calcrete and speleothem, have been widely used to date landscape change in karst environments, most commonly using U-series methods (^{230}Th/U, ^{231}Pa/^{238}U, ^{234}U/^{238}U, ^{206}Pb/^{238}U). At Pierre-la-Treiche, located along the entrenched Mosel valley into the Bajocian limestones (NE France), U-series ages of speleothems in fossil caves indicated that their growth was correlated to marine isotope stage (MIS) 6.5, 5.3, 3.3, 3.1, and 1 (Losson *et al.,* 2006). The U-series ages were used to identify several abrupt warming phases during MIS 3 - a cold period recorded in the Greenland ice cores and in the Grande Pile peat record from the Southern Vosges mountains, NE France (Pons-Branchu *et al.,* 2010). U-series analysis of pedogenic and groundwater calcrete horizons has also been used to constrain the timing of fluvial aggradation in karst settings such as the Sorbas basin of SE Spain (Candy *et al.,* 2015) and the limestone Orjen massif, western Montenegro (Adamson *et al.,* 2014), respectively.

A chronology based on multiple dating methods allows us to rigorously examine the relationships between fluvial evolution and karstification, where tiered travertine steps increase coherently with terrace age, or if there is a more complex terracing history involving cut-and-fil terraces, for example. A good example is the Tarn valley, near Millau (S France), where the dating framework has been a matter of debate (Ambert & Ambert, 1995). Based on the presumed ages of the travertine steps, the rate of incision of the Tarn Canyon was thought to be very low. However, recent OSL dating as well as palaeoecological and palaeontological analyses showed that the majority of travertine steps (Peyre) formed during MIS 5e-5b (Vernet *et al.,* 2008). This indicates that the incision rate in the Tarn valley has reached >30 cm/ka since the deposition of the ~75 ka-old terrace 3 (MIS 5b-5a), located 25 m above the valley floor. Secondary carbonate-based chronologies can be used alongside stable oxygen (δ^{18}O) and carbon (δ^{13}C) isotope ratio analysis to provide a record of interglacial climatic changes (Dabkowski *et al.,* 2011, 2016), such as interglacial tufas in France (e.g. La-Celle-sur-Seine, Paris Region: MIS 11 and Caours, Somme Basin: MIS 5e) and pedogenic calcretes in Southeast Spain (Adamson *et al.,* 2015; Gázquez *et al.,* 2016).

2.2. $^{26}Al/^{10}Be$ burial dating of cave-deposited alluvium

Burial dating is based on the differential decay of at least two cosmogenic nuclides (Granger and Muzikar, 2001). Amongst them, the pair $^{26}Al/^{10}Be$ is very well suited because: 1) both nuclides are produced in quartz, 2) their production ratio is fundamentally independent of latitude and altitude, and 3) it varies only slightly with depth (Dunai, 2010). Burial dating is useful in those settings where previously exposed quartz-bearing material (i.e. for $^{26}Al/^{10}Be$) becomes shielded from cosmic rays. Two basic assumptions must be fulfilled for a fast and complete burial (Granger and Muzikar, 2001). First, the time span over which incomplete shielding occurs is much shorter than the subsequent burial duration. Second, shielded sediments are buried deeply enough, i.e. in practice ≥30 m (rock equivalent mass), implying an insignificant production through muons at depth. We refer to the comprehensive works of Granger and Muzikar (2001), Dunai (2010) and Granger (2014) for further information about the basic principles of burial dating, including mathematical developments.

In the fluvio-karstic context, the burial event is achieved when river sediments, formerly exposed to cosmic rays at the Earth surface during hillslope denudation and fluvial transport, are washed into an underground system. The two aforementioned prerequisites are frequently met for in-cave deposited alluvium; the study of Granger *et al.* (2001) in Mammoth cave (i.e. the longest cave system known in the world, developed in Mississipian limestones in the Kentucky Appalachian Plateau) is one of the first successful applications of burial dating to such sediments. Since then, quartz-bearing material deposited into different multi-level cave systems by streams or rivers flowing into the sub-surface has been dated in a range of tectonically-active (e.g. Stock *et al.,* 2004) or moderately-uplifted (e.g. Anthony and Granger, 2007) settings. Inferring long-term river incision rates in these environments relies on the key assumption that the alluvium deposited in a horizontal, hydrologically abandoned, phreatic tube represents the last time the passage was at the local water table (Anthony and Granger, 2007). The selection of suitable sampling sites should ensure that abandoned and alluvium-filled phreatic tubes were not contaminated by any reworked material from an older (or younger) depositional episode (Dunai, 2010). It is therefore recommended to sample sediment layers displaying fluvial features or structures (Anthony and Granger, 2007) and/or where other material allows a cross-check with an independent dating method (e.g. U-series dating of a speleothem/flowstone sealing the fluvial sequence; Stock *et al.,* 2005).

In Europe, this approach, sometimes used in combination with paleomagnetism and U-series dating, was mostly applied to cave systems of mountainous environments: both in the Eastern (Wagner *et al.,* 2010; Häuselmann *et al.,* 2015) and the Western Alps (Häuselmann *et al.,* 2007; Hobléa *et al.,* 2011), and in the Pyrenees (Calvet *et al.,* 2015). Three case studies exemplify the value of burial dating of in-cave deposited alluvium to unravel long-term landscape evolution in diverse karstic environments (Fig. 2). First, the Têt valley (Eastern Pyrennées, France) shows nine karst levels, between 1400 to 400 m a.s.l., along its epigenetic fluvial gorge cut into the Devonian limestones of Villefranche de Conflent, with caves filled by sand and siliceous pebbles (Calvet *et al.,* 2015). Level 5 was dated from the lower Pliocene and level 3 from the Early Pleistocene, allowing an estimate of an incision rate of ~52 m/Ma, with a clear acceleration to 90 m/Ma for the last Ma. Level 3 is clearly linked to the upper terrace of the Têt valley and all the lower cave levels and sublevels strongly correlate to the younger terrace levels. Second, burial ages from different speleogenetic levels of the Siebenhengste-Hohgant cave system (Aare catchment, Switzerland) revealed a remarkable increase of glacial valley lowering since the beginning of the Middle Pleistocene, which substantially postdates the onset of glaciation in this region (Häuselmann *et al.,* 2007). This might be related to a considerable lowering of the equilibrium line altitude and the transgression of threshold conditions beyond which increase in glacial downcutting rates becomes nonlinear (Brocklehurst and Whipple, 2004). Third, burial ages coupled with magnetostratigraphy in multi-level cave systems along the Ardèche valley indicated a stepwise karst genesis during the Plio-Pleistocene, consistent with the *per ascensum* model of Mocochain *et al.* (2009), after the Messinian salinity crisis (Tassy *et al.,* 2013) especially, during the rise of sea level in the Lower Pliocene. These data also highlighted an uplift rate of ~30 mm/ka since 1.8 Ma in the lower Ardèche area.

2.3. Strengths and weaknesses of dating methods

Each numerical dating technique has an upper age limit (e.g. U-series: c. 350 ka; OSL: c. 150-200 ka; $^{26}Al/^{10}Be$ burial dating: c. 5.5 Ma) and associated analytical uncertainties. Ages obtained from adjacent karstic areas, or even within the same valley, can vary considerably. For example, in the Sierra of Atapuerca and the Arlanzón Valley (Moreno *et al.,* 2012) and in the upper Mosel catchment (Harmand & Cordier, 2012), TL, IRSL, ESR and U-series ages provided divergent results. In such instances, different ages may reliably represent spatial variations in uplift rates, river incision and karstification. However, it must be borne in mind

306 that these dating methods provide age information about different processes of landscape
307 evolution. Whereas burial ages give constraints about the last time the phreatic passage was at
308 the local water table, U-series ages date the timing of calcite formation and thereby provide
309 minimum ages of sediment deposition. A clear understanding of the chronostratigraphic
310 framework is therefore essential. Detailed geochronological studies, using multiple dating
311 methods, are required to reliably quantify rates of incision and karstification.
312
313 **3. Approaches for examining drainage evolution in karstic terrains**
314
315 The relationship between valley incision and karstification are summarized in Figure 3. Much
316 research has focused on the impacts of valley entrenchment on karst development, which can
317 in turn provide important insights into fluvial evolution. However, karst development can occur
318 independently of valley evolution, especially when dealing with the ghost-rock process (i.e.
319 rock transformation by self-volume chemical dissolution; Vergari & Quinif, 1997) or hypogene
320 karstification (i.e. dissolution and crystallization along ascending, often hydrothermal, flows;
321 Hill, 1987). A number of studies have highlighted the influence of karst terrain on valley
322 incision (Figure 3).
323
324 Analysis of the relationship between fluvial evolution and karstification requires a multiscale
325 approach, evolving from the valley bottom to the karst, and from the karst to the valley. This
326 review proposes a typology of relationships between karst and valley, depending on
327 morphostructural framework, lithology, base level change, and climatic fluctuations
328 (emphasizing the role of glaciers).
329
330 **3.1. From the valley bottom to the karst: relationships between karst cave level and valley**
331 **base level**
332
333 Many studies have highlighted the relationships between base level or cave level and the
334 regional evolution of river systems controlled by climatic, tectonic and/or eustatic forcing
335 (Ambert & Ambert, 1995; Jaillet, 2000; Audra *et al.,* 2001; Losson, 2003; Harmand *et al.,* 2004;
336 Wang *et al.,* 2004; Mocochain *et al.,* 2009; Guifang *et al.,* 2011; Ortega *et al.,* 2013; Tassy *et*
337 *al.,* 2013). As a result, it is well-established that karstic levels can provide valuable altitudinal
338 markers, or 'dip sticks' for river incision. This is especially effective in mountain massifs where

local relief can exceed several kilometers, and multiple cave levels exist, therefore providing long-term records of fluvial evolution since the Plio-Pleistocene.

Karst plays a major role in the formation and preservation of the fluvial sedimentary record. Where alluvial sediments accumulated in karst depressions, they became more immune to subsequent erosion and reworking (Delannoy, 1997; Audra *et al.,* 2001). Ancient alluvium is reported to have been preserved within karst settings since the Early Pleistocene (Wagner *et al.,* 2010; Adamson *et al.,* 2014; 2016); the Neogene (Hobléa *et al.,* 2011; Calvet *et al.,* 2015), the Paleogene (Bruxelles *et al.,* 2013) and even the Mesozoic (Vergari & Quinif, 1997), Palaeozoic (Osborne, 2007) and Precambrian (Buffard & Fischer, 1993). The excellent preservation potential of these records means that they are valuable archives of landscape change. This is especially the case where palaeovalleys or alluvial terraces are not well-preserved at the surface, when karstic cavities are disconnected from adjacent valleys, due to headward erosion (Enjalbert, 1967*, in* Nicod, 2010); or when there have been changes to drainage patterns (Adamson *et al.,* 2014). However, correlations between cave deposits and valley fills at the surface are sometimes difficult when karstic sediments are present only in isolated fragments, due to erosion and reworking of the exposed sediments (Quinif & Maire, 1998).

3.2. From the karst to the valley: Base level controls on the geometrical organization of karst drainage networks

Assuming that initial cave development occurs along the water table, Ford and Ewers (1978) proposed a conceptual framework called the "four-state model". In this model, different types of caves evolve depending on increasing fissure frequency through time: 1) bathyphreatic caves, with a few deep phreatic loops (Figure 2B.a, c, d); 2) phreatic caves with multiple and shallower loops (Audra & Palmer, 2011); 3) caves with a mixture of phreatic and water table-levelled components; and 4) an idealised water table cave without loops, formed as a result of high fissure frequency. The four-state model has been reinterpreted by Häuselmann (2002), Audra & Palmer (2011) and Gabrovšek *et al.* (2014) who pointed out two main controls in relation to valley incision: 1) The recharge control occurs in dammed aquifers, when recharge is fairly regular. Thus, the main endokarstic drain is established at the water table at the same altitude as the valley bottom (Figure 2B.b). When an irregular recharge occurs, looping tubes develop throughout the epiphreatic zone (Figure 2B.a). 2) The base-level control corresponds to the development of perched cave levels. Base level lowering is common in most temperate

climate karstic areas, especially mountainous regions, due to uplift of the continental crust and associated river incision (Figure 2A, Fig. 2B.c). In contrast, base-level rise produces flooded cave levels and Vauclusian springs, when water ascends (Figure 2B.c). Deep-phreatic cave systems, for instance, are located around the Mediterranean Sea, as a result of the Messinian marine regression and near instantaneous Pliocene flooding (Mocochain *et al.,* 2009).

3.3. A multi-scale approach

To effectively capture the complexity of karst evolution, and securely identify the relationships between fluvial activity and karstification, multi-scale analysis should be used to combine large-scale studies of karstified massifs and entrenched valleys, and local-scale analysis of individual karst drains and sediment fills. In valleys entrenched up to several hundred meters deep, numerous studies (Webb *et al.,* 1992; Audra *et al.,* 2001; Losson *et al.,* 2006; Guifang *et al.,* 2011; Rixhon *et al.,* 2014) have highlighted the altitudinal relationship between karstic passages and stepped terraces (Figure 2A). At the valley scale, establishing the elevation of alluvial terraces and karstic drains to within a few metres is sufficient for reliable geomorphological reconstructions. For example, in the Sierra de Atapuerca and the Arlanzón valley (Iberian Chain, Eastern Burgos, Spain), geomorphological analysis was combined with archaeology, palaeomagnetics, TL, IRSL, U-series and ESR dating to develop a chronostratigraphical framework of fluvial incision and speleogenesis of karst caves during the Lower and Middle Pleistocene (Moreno *et al.,* 2012; Ortega *et al.,* 2013).

At even larger spatial scales, across the Mediterranean basin for example, karstic and palaeovalley features suggest a common regional pattern of geomorphological evolution. At the Mediterranean coast, such as the South-East of France, Messinian canyons and Pliocene rias, among other features, demonstrate that sea level change has had a major influence on karstification (Audra *et al.,* 2004). Late Miocene base-level fall was followed by rising base-level in the Pliocene, which flooded lower endokarstic levels, and karst waters discharged as Vauclusian springs. In this system, higher elevation karst horizons are more recent forms, as indicated by *per ascensum* speleogenesis.

At smaller spatial scales, in individual caves or valleys, high-resolution analysis is essential when caves are disconnected from neighbouring valleys – due to erosion of the limestone valley sides or of terrace remains. For example, in the Pierre-Saint-Martin cave, Pleistocene deposits

of the Aranzadi gallery recorded a succession of depositional and entrenchment phases (Quinif & Maire, 1998). Three groups of speleothems situated between the detrital units highlighted the succession of several interglacial or interstadial stages allowing the precipitation of carbonate. U-series dating showed that speleothem growth occurred during MIS 9, 7 and earlyMIS 6. In the Têt river basin, recent research has provided precise correlations between aggradation and incision phases in each glacial cycle (Hez *et al.,* 2015; see section 5 for discussion).

4. A typology of the relationship between fluvial evolution and karstification

As outlined above, fluvial incision and karstification in limestones or evaporite rocks are driven by a number of factors. The most central are: eustasy, isostasy, climate and tectonics. Here we discuss the relationships between valley evolution and speleogenesis using examples from across Europe, as well as key studies in Australia, North America, and the Tibetan Plateau. Four models of valley evolution and karstification are proposed.

4.1. Karstification in association with base and cave level lowering

A number of karst systems have horizontal tubes and vertical conduits which reflect stability and incision in the neighbouring valleys, respectively. These valleys often contain stepped alluvial terraces associated with aggradation/incision cycles. Generally, epigenetic speleogenesis of limestone massifs and the succession of valley incision and aggradation are largely associated with strong isostatic or tectonic uplift. Climatic forcings have also played a key role, especially at the onset of the Quaternary, and during the Mid-Pleistocene Revolution at the onset of the 100 ka Milankovitch cycles (Bridgland *et al.,* 2009). Four types of geomorphological evolution are distinguished in the following discussion, based on the relief energy/topography of the karstified region.

4.1.1. Karstification in low elevation and very stable cratonic area

The Devonian limestone region of Buchan (South-East Australia) is a valuable example of slow, long-term incision and speleogenesis. Three fluvial terraces and epiphreatic cave levels have developed below a height of 30 m above the adjacent river (Webb *et al.,* 1992). Geomorphological evidence and palaeomagnetic dating indicate that these formed before 780 ka, giving a maximum incision rate of 38.5 mm/ka. The Buchan area has experienced only 4-5

m incision over the last 40 Ma (i.e. 0.1–0.125 mm/ka), 2-3 m of this has occurred over the last 730 ka (i.e. 2.7–4.1 mm/ka).

4.1.2. Karstification on low altitude plateaus (<500 m a.s.l.)

4.1.2.1. General cases

There are many examples of epigenetic speleogenesis and fluvial incision as a result of moderate (up to 10 mm/ka) uplift in cratonic areas, sedimentary basins, and low-altitude (<500 m-a.s.l.) basement plateaus, such as in the Paris, Aquitaine basins (Bridgland *et al.,* 2009; see *in* Audra, Ed., 2010) or British karst (Waltham *et al.,* 1997). In North America, the karst evolution of the Kentucky Appalachian Plateau has been dated in detail using TCN ages (Granger *et al.,* 2001). These karstic areas broadly correspond to one of two morphostructural settings. 1) Extended horizontal or monoclinal strata of Palaeozoic age (e.g. the Kentucky Plateau, USA: Granger *et al.,* 2001), Mesozoic or Cenozoic karstified rocks (e.g. in the plateaus of the Eastern Paris Basin, France; Jaillet, 2000; Losson, 2003; Devos *et al.,* 2007). 2) Folded strata in Alpine or older (e.g. Appalachian) structures. In most cases the caves are located in narrow outcrops of limestone, such as the Devonian and Carboniferous rocks of the Ardenne massif, Belgium (Quinif, 1999, 2006).

There have been several studies of Pleistocene sedimentary sequences from caves and river terraces formed on low-level plateaus (Losson, 2003; Jaillet *et al.,* 2004). These studies show that Pleistocene incision rates were low, and reached up to 100 mm/ka in the Mosel catchment (Harmand and Cordier, 2012). On low-elevation karst plateau, there is evidence for Quaternary rejuvenation of older palaeo-karsts or crypto-karsts, such as the Belgian Ardenne, Eastern Paris Basin, and Quercy plateaus (Bruxelles *et al.,* 2013; Vergari and Quinif, 1997; Harmand *et al.,* 2004). At Poissons (Eastern Paris Basin, France), Pleistocene incision of the upper Marne reached 42 mm/ka to 58 mm/ka, and extended below the base of the palaeokarstic wells, which were filled with continental Infra-Cretaceous (Wealdian) ferruginous deposits (Harmand *et al.,* 2004). However, the presence of Late Pleistocene fauna and MIS 6 speleothems in the sediment fill (Jaillet, 2000) was indicative of a Quaternary karstification of the older palaeo-karsts.

4.1.2.2. The relations between rivers, aquifers and karst in the Eastern Paris basin

In the Eastern Paris Basin, epigenetic speleogenesis and fluvial incision is linked to the structural framework of the basin and entrenchment of the main valley into the alternating marl and limestone strata (Losson, 2003; Devos *et al.,* 2009, 2015). The main feature is the position of the river with regard to the water table. Four situations can be distinguished (Figure 4A). 1) When perched rivers are entrenched into limestone above the saturated zone, infiltration occurs into and under the valley from local or allochtonous flows (Jaillet, 2000; Losson, 2003; Devos *et al.,* 2009, 2015; Figure 4A level a). 2) When the surface river channel is in contact with the water table of the saturated zone, the lack of hydraulic gradient induces a ghost rock process around the fractures of the valley floor (Quinif, 2010, Devos *et al.,* 2011; Figure.4A level b). In contrast, lowering of the piezometric level, due to fluvial incision, causes the discharge of residual deposits of the ghost rocks and the creation of conduits in the epiphreatic zone. 3) When the surface river channel is strongly entrenched into the limestone substratum, and drains the flooded karst zone, a thin piezometric horizon develops (Figure 4A level c). 4) If fluvial incision occurs in the marls or clays situated below the saturated zone, the perched karstified zone is disconnected from the river (Figure 4A level d) and the flooded zone drains into low flow springs (Devos *et al.,* 2015). However, as shown in Figure 4B, it is important to remember that the faulted tectonic basement can produce structural and aquifer compartments which control the hydraulic gradient between aquifers and rivers (Devos *et al.,* 2007).This can have major impacts on the hydrological and geomorphological connectivity, between karst and subaerial fluvial drainage networks.

4.1.3. Relationships between fluvial incision/aggradation and karstification on high altitude plateaus and low mountain ranges (500 – 2,000 a.s.l.)

In low mountain ranges and high plateaus, a moderate uplift rate (up to 100-200 mm/ka) commonly causes deep fluvial incision and epigenetic speleogenesis in thick limestone strata. On some high plateaus, geomorphological processes have continuously shaped the landscape since the Neogene. In the Southern part of the Causse of Larzac, four stages of speleogenesis were identified from the Middle Miocene until the Pliocene (Camus, 1997, 2010). Even during the Pleistocene, there is evidence of phases of incision and karstification in many regions, such as the Sierra de Atapuerca and the Arlanzón valley (Moreno *et al.,* 2012; Ortega *et al.,* 2013), the Languedocian plateaus (Audra *et al.,* 2001) or the Swabian Alb (Abel *et al.,* 2002). These speleogenetic phases occurred in response to base-level and cave-level lowering, due to tectonic uplift and glacially-driven sea level change. During Pleistocene glacial stages, sea level fell by

up to 140 m below modern levels (Rohling *et al.,* 2009). In some settings, such as the Arlanzón and Ardèche valleys, incision has reached over 100 m deep since the Lower Pleistocene. The number of terrace levels varies between the narrow middle Ardèche valley (4) and the wide Arlanzón valley (14), but the karstified massifs exhibit only 2 or 3 cave levels, respectively (Audra *et al.,* 2001; Moreno *et al.,* 2012; Ortega *et al.,* 2013).

4.1.4. Long-term records of fluvial incision and karstification in high mountain regions (>2,000 m a.s.l.)

Many high altitude limestone mountains contain horizontal cave networks at elevations exceeding 2,000 m a.s.l. (Feichtnerschacht, Austrian Alps: 2,000 m; French subalpine chains: 2,300 m; Dolomites, northeastern Italy: 2,775 m; Siebenhengste-Hohgant-Höhle, Berner Oberland, Switzerland >2,000 m; Häuselmann and Granger, 2005; Audra *et al.,* 2007; Wagner *et al.*, 2010, Hoblea *et al.*, 2011; Figure 5A). Many of these mountains contain thick horizons of karstified rock that extend vertically for up to 1 km, and are characterized by cave to rock ratios as high as 1.3 m^3 per 1000 m^3. Some high mountains also contain long karstic cavities (up to 90 km in the Granier massif, Grande Chartreuse, France, Hoblea *et al.,* 2011) and many cave levels (9 in the Têt catchment; 14 in the Siebenhengste; Calvet *et al.,* 2015; Häuselmann, 2002). These stacked caves indicate numerous speleogenetic phases and strong uplift trends. Where these endokarstic galleries contain alluvial sedimentary sequences, they have the potential to record long-term fluvial evolution. Key examples include the European Alps (Styrian Alps: Wagner *et al.,* 2010; Grande Chartreuse massif: Hoblea *et al.* 2011), the Alpi Apuane, Italy (Piccini *et al.,* 2011), the Sierra Nevada, California (Stock *et al.,* 2004, 2005), and the Hengduan Shan, Tibet (McPhillips *et al.,* 2016).

In the Alps and Pyrenees, TCN burial dating of sediment infills from the highest cave levels frequently yielded Pliocene ages (Häuselmann and Granger, 2005; Wagner *et al.,* 2010; Hoblea *et al.,* 2011; Calvet *et al.,* 2015). The same method, based on the ^{10}Be and ^{21}Ne isotope pair, revealed a Lower Miocene karstification age at the Southeast margin of the Tibetan Plateau at the First Bend (McPhillips *et al.,* 2016). Valley incision and karstification continued during the Quaternary period in European karst regions (Häuselmann and Granger, 2005; Wagner *et al.,* 2010; Calvet *et al.,* 2015), and in China (Qinling: Wang *et al.,* 2004; Northwestern Hunan: Guifang *et al.,* 2011; Guizhou plateau: Liu *et al.,* 2013).

543 Many high altitude karstified massifs, including the limestone mountains of Europe (e.g.
544 Hughes *et al.,* 2010) and North America (Palmer and Palmer, 1993), were glaciated during
545 Pleistocene cold stages, including MIS 12, 6, and the Younger Dryas. As a result, they evolved
546 into a distinctive 'glaciokarst' landscape (See section 4.3).
547
548 **4.2. Karstification in association with rising base and cave level**
549
550 The *per ascensum* model of speleogenesis is initiated by eustasy and climatically-driven
551 aggradation and subsidence (Audra *et al.,* 2001; Figure 5B). The influence of eustatic base level
552 does not typically extend more than 200 km inland (Antoine *et al.,* 2000). In Europe, one of the
553 most significant examples of rising base level and its impacts on terrestrial landscape change is
554 the Pliocene transgression after the Messinian regression of the Mediterranean basin (e.g.
555 Clauzon, 1978; Audra *et al.,* 2004).
556
557 The Languedocian plateaus, incised by the Lower Ardèche canyon (at Saint-Remèze), present
558 a record of rising base and cave level since the Messinian. TCN dating combined with
559 magnetostratigraphy revealed that, following an early phase of karstification during the
560 Messinian regression, subsequent phases of speleogenesis took place during marine and
561 continental aggradation in the Pliocene rias (Mocochain *et al.,* 2009; Tassy *et al.,* 2013, 2014).
562 Rising base level caused flooding of the lower cave levels, which discharged as Vauclusian
563 springs. Pleistocene valley incision led to the progressive draining of horizons situated above
564 base level and the reactivation of caves at the same altitude as the river.
565
566 Other cases of base and cave level fluctuations follow a similar evolutionary model (Bruthans
567 and Zeman, 2003; Audra and Palmer, 2011). Several cases of *per ascensum* speleogenesis by
568 fluvial (or glacial) aggradation occur in Europe, including Podtraťová jeskyně in the Moravian
569 karst (Czech Republic, Bruthans and Zeman, 2003) and in the Devoluy mountains, France
570 (Audra & Palmer, 2011). In the Devoluy chain, the Pleistocene glacial, lacustrine, and
571 glaciofluvial sediment fill increased the elevation of the Gillardes karst springs, and caused the
572 300 m high chimney shaft at Puits de Bans to overflow.
573
574 **4.3. Pleistocene incision and karstification in association with glaciation**
575

Broadly, there are three mechanisms through which Pleistocene glacial activity influenced karst areas. First, in non-glaciated mountains or plateaus areas, incision and karstification were indirectly conditioned by glacial activity, such as the Kentucky Appalachian Plateau (Palmer and Palmer, 1993). Second, in glaciated mountain regions, such as parts of the Dinaric Alps in Montenegro (Hughes *et al.,* 2010; 2011; Adamson *et al.,* 2014), and the Pindus mountains in Greece (Hughes *et al.,* 2006; Woodward *et al.,* 2008), fluvial evolution and karstification were directly influenced by glaciers. Third, some karst areas were covered by ice sheets up to 3 km thick that developed across much of Northern Eurasia (Eurasian Ice Sheet) and North America (Laurentide Ice Sheet) during Pleistocene glacial phases. The erosional effects of the ice sheets on karst and non-karst landforms and deglacial speleogenesis, are beyond the scope of this paper, which concentrates on karst geomorphology south of the major ice-sheets, and downstream of ice caps and valley glaciers (mechanisms one and two outlined above).

4.3.1. Indirect impacts of glaciation: the Appalachian plateau of Kentucky, USA

The Kentucky Appalachian Plateau (c. 2,000 m a.s.l.) is a vast karstified area that contains an extensive sinkhole plain (Pennyroyal Plateau) and the Mammoth Cave Plateau where the famous cave provides a well-preserved example of the indirect influence of glaciers on Plio-Quaternary morphologic evolution (Palmer and Palmer, 1993). TCN (^{26}Al and ^{10}Be) dating of sediments in the five levels of Mammoth Cave, as well as vertical vadose passages, is in accordance with the timing of Pliocene and Pleistocene glaciations of North America (Granger *et al.,* 2001). Major aggradational phases occurred at c. 3.2, 2.3 and 0.8 Ma, when large volumes of sediment would have been produced by the ice sheet and delivered downstream via meltwater channels. A major incision phase occurred at c. 1.39 Ma in relation to a drainage change towards the Mississipi catchment when the Ohio river formed along the Southern North-American ice-sheet margin.

4.3.2. Direct impacts of glaciation: Glaciated limestone mountains: examples from the Dinaric Alps

Limestone mountains that were glaciated by ice caps or valley glaciers during Pleistocene cold stages, such as the Dinaric Alps, are characterized by a distinctive ‘glaciokarst’ terrain, which displays features including limestone pavements and bare bedrock surfaces. The presence of glaciers in karst environments can have major impacts on glaciofluvial drainage pathways, and

subsequent karst drainage evolution. On the Orjen massif in western Montenegro, a large ice cap developed during the Pleistocene (MIS 12, 6, 5d-2 and the Younger Dryas, Hughes *et al.,* 2010). The configuration of the Orjen massif, with its high altitude (c. 1,800 m a.s.l.) ice accumulation zone, and surrounding depocentres (such as valleys, poljes and dolines), meant that during the major ice advance of MIS 12, ice extended over the plateau, and likely plugged the surface of karst depressions and conduits. Meltwater was delivered directly downstream and largely flowed at the land surface. This is evidenced by the presence of large volumes of glaciofluvial sediments that have been deposited and preserved in large poljes, as terraced valley fills, and as alluvial fans at the margins of the plateau (Adamson *et al.,* 2014; 2016a). One of these alluvial fans, the Lipci fan, extends offshore into the Bay of Kotor. It was deposited subaerially at the southern margins of the Orjen massif during the major glacial phase of MIS 12, when sea level in this part of the Mediterranean was up to 140 m lower than present, and the Bay of Kotor was exposed subaerially (Adamson *et al.,* 2016b). U-series ages of the alluvial deposits at Orjen are consistent with the timing of glacial activity (Hughes *et al.,* 2010). During subsequent cold stages (MIS 6, 5d-2, and the Younger Dryas), the ice cap did not advance beyond the plateau. During these periods, large areas of karst were exposed on the plateau, and meltwater was channeled into subterranean cavities (Adamson *et al.,* 2014). There is only limited evidence of post-MIS 12 alluvium preserved at the surface of the Orjen massif, and incision into the sediment fills is negligible. As a consequence, the oldest (Middle Pleistocene) part of the alluvial record is exceptionally well-preserved, but the youngest archives are not accessible at the surface. The interactions between glacial activity, karst terrain, and fluvial pathways, can therefore be a major control on the Quaternary sedimentary record in such glaciated regions (Stepišnik *et al*., 2009; Adamson *et al.,* 2014).

4.4. The particular case of karstified evaporites

In evaporite rocks, karst systems are sparser and tend to be restricted to relatively drier climate regions due to the restricted availability of moisture. However, in such environments the preservation potential of karst systems is much higher. In some regions of evaporitic bedrock, most commonly gypsum, climate forcing in uplifting areas generates cave levels associated with patterns of river incision and aggradation. In the Northern Apennines, Italy, especially in the region of Emilia Romagna, the Re Tiberio cave system is hosted in Messinian gypsum (Columbu *et al.,* 2015). Gypsum is much more soluble than limestone, and cave levels form very rapidly.

644 Two significant examples of karstified evaporites also exist in Spain, in the Sorbas basin,
645 Southeastern Spain, and in the Gállego valley, in the central Ebro Basin, with cave levels and
646 subsidence areas respectively (Calaforra and Pulido-Bosch, 2003).
647
648 **4.4.1. Cave levels in karstified evaporites**
649
650 The Sorbas basin, Southeast Spain, contains an interstratal karst system formed within
651 intercalated Messinian gypsum and marls (Calaforra & Pulido-Bosch, 2003; Figure 6A). At
652 first, the gypsum karst evolved under phreatic conditions during the early Pleistocene, enabling
653 the formation of small conduits. Subsequently, mechanical erosion occurred under vadose
654 conditions. Increased incision, as a consequence of rapid Plio-Pleistocene uplift (>80-160
655 mm/ka; Mather, 2000) allowed an eastward capture of the Upper Aguas river system at c. 70
656 ka (based on U series dating of river terrace calcretes, Candy et al., 2005, Harvey *et al.,* 2014).
657 Dated pre-capture terraces represent the former southern drainage system of the Rio Aguas,
658 prior to the river capture event, enabling incision rates to be calculated (Stokes *et al.,* 2002). In
659 fact, the capture leads to a 10 fold increase in incision rates, driven by the ~90m base level drop
660 that it initiated (Stokes *et al.,* 2002). This incision led to the development of further cave levels.
661 Karst tributaries that were connected to the Aguas channel at the surface, were protected from
662 enhanced incision due to the development of the cave network (Mather 2000). Headward
663 incision in the Upper Aguas catchment induced a lowering of the piezometric level in the Sorbas
664 basin. Subterranean erosion processes, largely concentrated into the marl strata, occurred under
665 vadose conditions (Calaforra & Pulido-Bosch, 2003), and these processes continue at the
666 present day.
667
668 **4.4.2. Subsidence in evaporite rock areas**
669
670 Bruthans and Zeman (2003) identified a suit of features typical of salt karst terrain, including
671 broad and low caves shaped by subterranean meandering streams, and the development of large
672 subterranean alluvial fans, due to the high solubility of salt (NaCl). Apart from these forms, a
673 key feature of evaporite karst (e.g. gypsum karst) is the incomplete record of valley evolution
674 due to high solubility and enhanced dissolution and subsidence. A number of examples exist
675 worldwide, most notably in Spain (Benito *et al.,* 1998, 2010; Figure 6B). In the Gállego valley,
676 in the central Ebro Basin, Northern Zaragoza, 12 stepped terraces (2-5 m thick) were mapped
677 upstream of Zuera. Downstream, the complex of alluvial formations is over 100 m thick. This

downstream thickening of the alluvial formations, as well as multi-scale karstic depressions and syn- and post-sedimentary deformations, such as collapses, reverse faults, and marl-clay diapiric structures, reflect the dissolution of Cenozoic evaporitic bedrock. Palaomagnetic and OSL dating revealed two main periods of subsidence and associated alluvial aggradation: the first (represented by terraces T2, T3, and T4) began in the Early Pleistocene (Benito *et al.,* 1998). The second occurred during MIS 6, primarily when glaciers were present in the Pyrenees. A later phase also occurred during the Warthe Advance, a later part of MIS 6 (155-140 ka), as a result of high discharge delivered by the upper catchment of the Gállego River (Benito *et al.,* 2010).

In the Eastern Cinca and Segre catchments of the Ebro Basin, Lucha *et al.* (2012) identified a phase of dissolution subsidence and halokinetic uplift along the evaporitic core of the Barbastro–Balaguer Anticline. Eight of the nine fluvial terraces were affected by dissolution-induced synsedimentary subsidence, by dissolution-induced post-sedimentary subsidence, or by deformation due to salt flow, especially the upper Pleistocene terrace 4 of the Cinca River. OSL ages obtained in the alluvial sediments of this backtilted terrace indicated a minimum uplift rate of 0.3 mm/a (Lucha *et al.*, 2012). Moreover, deposits of the highest terrace levels reach over 100 m thickness in the Segre catchment, in basins generated by dissolution-induced synsedimentary subsidence.

5. Discussion

5.1. Variability of incision rates in karst fluvial systems

Based on chronological evidence from karstic fluvial sedimentary fills and secondary carbonate forms, such as travertine and calcrete, long-term regional incision rates can be securely constrained. In fact, numerical dating highlights the variability in space and time of river incision rates. Incision rates are highest in high mountains (>2,000 m a.s.l.), exceeding 100 mm/ka in the Alps (Hobléa *et al.,* 2011; Häuselmann & Granger, 2005; Wagner *et al.,* 2010) or in China (especially on the southeast margin of the Tibetan Plateau, McPhillips *et al.,* 2016). Incision rates are lower (<100 mm/ka) in the plateaus and low mountain range areas (200-2,000 m a.s.l.), such as the Eastern Paris Basin (Harmand & Cordier, 2012), the Languedocian plateaus (Ambert & Ambert, 1995; Camus, 1997; Audra *et al.,* 2001), the Duero basin (Moreno *et al.,* 2012; Ortega *et al.,* 2013), Swabian Alps (Abel *et al.,* 2002), or the Eastern Pyrenees

712 (Calvet *et al.,* 2015). The lowest incision rates (typically <10 mm/ka) are measured in
713 Palaeozoic crustal provinces, such as the Southeastern part of Australia (Webb *et al.,* 1992) or
714 on the Appalachian plateau (Granger *et al.,* 2001).
715
716 Most of the time, higher incision rates are related to periods of stronger uplift, such as in the
717 Styrian Alps or the Western American Sierra Nevada, where Miocene uplift rates reached 140
718 mm/ka (Stock *et al.,* 2005; Wagner *et al.,* 2010). Where karstification and fluvial dynamics
719 have been studied in particular detail, it is possible to identify multiple uplift phases during the
720 Cenozoic era. This is the case in the Languedocian plateaus where karstic and valley evolution
721 corresponded to several uplift pulses since the Cretaceous period (Séranne *et al.,* 2002); the last
722 pulse occurring during the Middle to Late Miocene. The onset of accelerated incision is related
723 to Pliocene and Pleistocene tectonic uplift and climate change, in the Sierra Nevada (from 3
724 and 1.5 Ma; Stock *et al.,* 2005), in the middle Ardèche valley (since 2 Ma; Audra *et al.,* 2001)
725 or in the Eastern Pyrenees (since the beginning of the Pleistocene; Calvet *et al.,* 2015).
726 Variations in tectonically- and climatically-driven incision rates are conditioned locally by
727 geomorphology and fluvial behavior, such as river capture. In the Styrian Alps, strong incision
728 of the Mur River, from 4 to 2.5 Ma was connected with an extension of the Mur catchment
729 following river drainage change (Wagner *et al.*, 2010). Decreased incision during the
730 Quaternary corresponded to fluvial aggradation during Pleistocene cold periods and reduced
731 potential for bedrock entrenchment. Short-term increase in incision rate in the Siebenhengste at
732 800 ka has been related to a change in flow direction from the Eriz valley to the south, to the
733 Aare valley in the north (Häuselmann & Granger, 2005). Similar short-term changes in incision
734 rate are evident in the Mammoth Cave record, where an incision event at c. 1.4 Ma has been
735 correlated with headward erosion in the Green River valley, after the formation of the Ohio
736 River, at the end of an ice-sheet advance (Granger *et al.,* 2001).
737
738 Delayed response between tectonic uplift and resulting fluvial incision can also be discerned
739 from the karst-fluvial archive. This is the case in the Ardenne massif where ^{10}Be dating
740 highlighted diachronous river incision from the lower Meuse valley at the northern rim of the
741 Ardenne to its intra-massif (sub–) tributaries, i.e. Belle-Roche in the Amblève valley (Rixhon
742 *et al.*, 2011, 2014). However, rates of knickpoint retreat are variable, and depend on many
743 factors, including climate, discharge, lithology, tectonics and time (Whittaker & Boulton,
744 2012). These controls are translated into the morphosedimentary record as spatial variations in
745 the timing of uplift, valley incision, aggradation, and karstification. In the Upper Yangzi

746 catchment, cosmogenic nuclide ages suggest a considerably delayed response (c. 20 Ma)
747 between Late Eocene uplift (Hoke *et al.,* 2014) and Miocene incision (from 18 to 9 Ma), such
748 that valley incision is not a useful proxy for surface uplift (McPhillips *et al.*, 2016).
749
750 **5.2. Models of valley evolution and karstification**
751
752 At the regional scale (e.g. across the Mediterranean basin), eustatic, isostatic, tectonic and
753 climatic factors, largely explain the rise or fall of base and cave levels. These drivers do not
754 influence hypogenic caves and ghost rocks (isovolumetric weathering with very low flow)
755 because these types of speleogenesis are not connected to a fluvial base level. However, uplifted
756 hypogenic and ghost rock karsts can be reactivated, as cryptokarsts (when karstification occurs
757 under an impervious sedimentary cover) or palaeokarsts, when they can be influenced by base
758 and cave level change (e.g. Wealdian: continental Infra-Cretaceous (Vergari & Quinif, 1997;
759 Jaillet *et al.,* 2004). In most karst regions, geomorphological evolution consists of valley
760 incision and *per descensum* speleogenesis. Over Quaternary timescales, this model is
761 underpinned by climate change, since tectonic uplift and subsidence change over much longer
762 geological time spans. Thus, Quaternary glacial and interglacial cycles are recorded in terraces
763 and caves by aggradation, incision, or concretion phases (Antoine, 1994; Quinif, 2006;
764 Columbu *et al.,* 2015).
765
766 At the catchment scale, Pleistocene climatic cycles and geomorphological factors influenced
767 fluvial and karstic environments. In many catchments, river incision chiefly occurs during cold-
768 to-warm or warm-to-cold climatic transitions, in accordance with regional climate change
769 (Antoine, 1994; Bridgland *et al.,* 2009). Underground streams adjust to falling base level by
770 incising new passages. However, there is evidence that *per descensum* speleogenesis also
771 depends on the timing of valley incision, as well as geological factors such as (i) the degree of
772 bedrock karstification (Abel *et al.,* 2002), (ii) alternating pervious and impervious strata causing
773 perched karsts (Devos *et al.,* 2015, Figure 4A level a) and iii) underground karstic flows towards
774 a lower elevation river in a neighbouring hydrographic basin or in the downstream position of
775 the same river (Losson, 2003). As a consequence, numerous interactions between fluvial
776 evolution and karstification can exist. We therefore propose four local to regional models of
777 Quaternary geomorphological evolution from different settings: 1) Eastern Pyrenees, in
778 limestone rocks, 2 and 3) low limestone plateaus of the Eastern Paris Basin and 4) a rapidly-

779 uplifted gypsum area in the Northern Apennines, Italy (Losson, 2003; Antoine *et al.,* 2006; Hez
780 *et al.,* 2015; Colombu *et al.,* 2015).
781
782 **5.2.1 A conceptual model of valley scale karstic and fluvial development: river terrace**
783 **records in the Têt basin (Eastern French Pyrenees)**
784
785 On the basis of river terrace records from the Eastern French Pyrenees (Calvet *et al.,* 2015; Hez
786 *et al.,* 2015), a valley-scale conceptual model of karst drainage evolution is presented in Figure
787 7. This reflects changes in karst genesis, evolution, and abandonment as well as fluvial incision
788 into bedrock, sediment aggradation, and terrace incision/abandonment. This model is based on
789 cavities in the Têt basin, especially in the Devonian limestones syncline of Villefranche, where
790 nine horizontal conduits exist up to 1,000 m above the present valley floor (Hez *et al.,* 2015;
791 Calvet *et al.,* 2015). The two lowest karstic tubes contain rich morphologies of sediment fill
792 and corrosion forms, which can be explained by the succession of three genetic karstic phases
793 (Figure 7A, C). In phase 1, the presence of phreatic caves indicates syngenetic karstification
794 below base level during or after valley incision. In phase 2, bench walls and the corroded ceiling
795 of the horizontal conduit indicate aggradation at the valley bottom leading to progressive and
796 synchronous base-level rise during a paragenetic phase. During phase 3, funnel shaped conduits
797 cutting down into the horizontal tubes highlight a period of renewed incision ("trepanning",
798 Jaillet *et al.*, 2004). This suggests a diachronic evolution of the caves with: a) lowering of the
799 base-level inducing downstream incision of the paragenetic stage sediments. Thus, ancient
800 horizontal conduits shaped in the flooded zone evolve downstream in the vadose zone where
801 the cave deposits are partially reworked (see phase 1); b) formation of bench walls in the middle
802 part of the galleries; and c) deposition of a cave fan delta upstream. Indeed, a strong hydraulic
803 gradient (1/1000) and flooding on the perched valley floor causes upstream transport and
804 deposition of coarse alluvium in karstic caves. In a last stage d), headward erosion along the
805 valley axis induces fluvial incision of the alluvial plain and underlying bedrock, and
806 entrenchment of the cave fill. Beneath the valley floor, a karstic drain is initiated in the flooded
807 zone (Figure 7B).
808
809 One must note that this model of karstic drain evolution and the relationships between valley
810 and karstic development during a Pleistocene climatic cycle is not valid when underground flow
811 is diverted to stream capture or piracy (see below, Figure 8B). Thus, in the capture area of the

812 Moselle river by the Meurthe (Losson, 2003), the caves of Pierre-la-Treiche show that the
813 endokarstic networks are not correlated in elevation with the Moselle terraces.
814
815 **5.2.2. Two conceptual models of regional karstic and fluvial development in low limestone**
816 **plateaus: cave records**
817
818 In limestone plateaus, alluvial stepped terraces and tiered cave infills record successive
819 Milankovitch cycles of palaeoenvironmental change (Figure 8). In both models (Figure 8A and
820 8B), two positions are distinguished based to the type of speleogenesis. Figure 8A shows the
821 evolution of a plateau karst where the caves are in connection with the valley bottom. Figure
822 8B presents a valley karst. The lower caves, situated below the water table, are in connection
823 with the base level of another valley which is located below the water table, as in Pierre-la-
824 Treiche (Losson *et al.,* 2006). Figure 8B3 presents a valley karst where underground flows
825 occur between zones of karstic losses and resurgences along the same valley, such as the upper
826 Meuse upstream of Neufchâteau, Eastern Paris basin (Losson, 2003).
827
828 In both models, stage 1 corresponds to an interglacial period with pedogenesis and silt
829 deposition in river systems and caves. Biological CO_2 allows speleothem, travertine and tufa
830 growth, especially in warm environments or in chalk Cretaceous catchments where thick tufa
831 deposits occur (Antoine *et al.,* 2006, Figure 8A). During stage 2, at the onset of climate cooling,
832 the progressive disappearance of forests leads to soil erosion on the slopes, lateral erosion in
833 the meandering valleys, and headward erosion of the steep slopes of the karstic massif (Antoine,
834 1994). As a consequence, cave entrances become disconnected from the valley bottom in a
835 plateau karst (Figure 8A). There is little or no speleothem growth in vadose caves and fine
836 clastic deposits (from soil erosion) are deposed in flooded cavities. Lower flooded caves are
837 situated below the water table in relation to neighbouring valley (such as the Palaeo-Meurthe
838 valley, Figure 8B). In the cold period (stage 3), for example in the Moselle valley (Figure 8B),
839 the river entrenches into the bedrock, above the former flooded caves connected with the
840 Palaeo-Meurthe river. In stage 4, during full glacial conditions (such as the Last Glacial
841 Maximum, MIS 2), coarse alluvium, originating from the glaciated Vosges massif, was
842 deposited by a braided river in the valley bottom. This material was also deposited in the lower
843 elevation flooded or vadose caves (Losson *et al.,* 2006). In fact, glaciated karst regions where
844 a major glacial advance occurs generates large volumes of sediment that are deposited in karst
845 cavities at the surface and subsurface, leading to major phases of aggradation

(e.g. Lewin & Woodward, 2009; Adamson *et al.,* 2014, 2016a and b). No speleothem formation occurs during full glacial conditions (Fairchild and Baker, 2012).

When large volumes of alluvium are deposited on the valley floor, they can fill caves that are situated (almost) at the same altitude as the river (Figure 8A), such as the Middle Pleistocene filling of the Belle-Roche cave in the Ardenne massif (Rixhon *et al.,* 2014). Some authors have highlighted the difference between wet glacial periods characterized by sediment-laden rivers, and dry cold periods with reworked loess, for example in Belgian caves, close to the former margins of the Fennoscandian ice sheet (Quinif, 2006). Where caves have become filled, they display evidence of a complex geomorphological evolution, with successive phases of aggradation and incision (Quinif & Maire, 1998).

The wide caves of Pierre-la-Treiche, filled with coarse grained alluvium (Figure 8B) indicate a speleogenetic phase during an interglacial period, before the deposition of alluvium in the subsequent glaciation. However, the horizontal cave levels of the (epi)phreatic zone, which correspond to stable base levels without tectonic uplift, require a minimum formation time by solutional processes of 10-40 ka (Ford & Williams, 1989). The time period between two Quaternary glaciations (MIS 5e, c, a) is thus long enough for dissolution processes to excavate the horizontal tubes. During the subsequent interglacial, new flooded caves were formed at the bottom of the valley where tufa deposits can develop (Antoine *et al.,* 2006; Dabkowski *et al.,* 2011; Figure 8A). Today, at Pierre-la-Treiche, the entrenched valley of the Moselle is situated below the vadose caves (Losson, 2003; Cordier *et al.,* 2006) where speleothems have grown since 300 ka, spanning several interglacial and interstadial periods (Losson, 2003, Losson *et al.,* 2006; Pons-Branchu *et al.,* 2010).

5.2.3. Model of climate-driven speleogenesis of gypsum caves

Figure 9 presents a model of climate-driven river incision and karstification based on the multi-level gypsum cave systems of the Re Tiberio (Fig. 1) situated in the moderately-rapidly uplifted Northern Apennines, Italy (Columbu *et al.,* 2015). This Italian karstified area presents a more relevant model than the Spanish karsts, where the subsidence is irregular in time and space (Gállego valley) or where the geomorphological evolution is accelerated by a river capture event (Rio Aguas, Sorbas basin, see 4.4). Mostly, in the Re Tiberio valley, dating speleothems provide a more precise chronological framework (Columbu *et al.,* 2015). U-series ages of

880 calcite speleothems from the three cave levels, situated at 340, 215, and 190 m a.s.l., revealed
881 growth phases during the MIS 5e, MIS 5d-c (Dansgaard-Oeschger cycle 24) and MIS 5b-a (D-
882 O cycles 22 to 20), respectively. The ages suggest rapid entrenchment during cold periods,
883 because uplift rates had reached c. 1 mm/yr since the end of the Middle Pleistocene (Columbu
884 *et al.,* 2015).
885
886 This model presents significant differences with previous conceptual models (see Figs 7 and 8),
887 because horizontal cave levels formed during cold periods. Karst evolution was rapid,
888 especially during wetter phases, due to increased bedload (Figure 9B2, 9B3, 9B4). Valley
889 aggradation led to the infilling of cave passages and a paragenetic karstification due to slowly
890 rising base level. During the subsequent warm period, decreased bedload initiated incision into
891 the cave sediments, but karstification was slow (Figure 9A, 9B5). The key similarities with the
892 models presented in Figures 7 and 8, are that carbonate speleothems grew during wet and warm
893 interglacials or interstadials (MIS 5e, 5d-a, 5b-a, figure 9A, 9B1) and valley incision occurred
894 at cooling transitions due to high stream discharge and low bedload concentrations (figure 9B2).
895
896 **5.2.4. Diverse models of karstic and valley evolution**
897
898 The four models outlined above present idealised scenarios, based on existing evidence, but
899 more complex models of fluvial and karstic evolution can occur in response to local to regional
900 conditions. Thus, successive aggradation or erosion phases can occur over multiple cold
901 periods. These can be recorded in the same cave level, as in the Pierre-Saint-Martin caves in
902 the French Pyrenees (Quinif & Maire, 1998). On the other hand, tiered caves can be filled with
903 deposits of the same age, as in the Mammoth cave, USA (Granger *et al.,* 2001). Establishing
904 the model of karst and valley evolution in different settings relies on the number of cave levels
905 and river terrace surfaces in a connected valley. However, the number of cave passage levels
906 present in karst landscapes is commonly lower than the number of 100 ka cycles that have
907 occurred over the last 1 Ma of the Quaternary. This suggests that karst-fluvial systems might
908 record only the major climate changes ('supercycles' of Kukla, 2005; Bridgland *et al.,* 2009)
909 or/and variations in uplift rate.
910
911 **6. Conclusion**
912

For two decades, analysis of river systems in karstic areas, including the wider application of dating methods, such as cosmogenic nuclide dating of cave infills, have provided a better understanding of geomorphological evolution over the Cenozoic era, especially during the Quaternary. Alluvial records in karst terrain, especially in European karst catchments, where the sedimentary records are particularly well preserved compared to their sub-aerial counterparts, now provide a reliable record of landscape evolution that can be effectively tied to wider, regional morphosedimentary archives.

Evidence indicates that many factors, including uplift, eustatic fluctuations, climatic conditions and fluvial dynamics (e.g. knickpoint retreat, increased channel flow and/or sediment load, and stream piracies), can play a major role in speleogenesis and geomorphological evolution. Data reviewed here have allowed us to propose a four-fold typology of the relationship between fluvial evolution and karstification: 1) karstification in association with base and cave level lowering, i) in low elevation and tectonically-stable cratonic area, ii) on low altitude plateaus (<500 m a.s.l.), iii) on high altitude plateaus and low mountain ranges (500 – 2,000 a.s.l.), where long-term records of fluvial incision and karstification are present; iv) in high mountain regions (>2,000 m a.s.l.), 2) karstification in association with rising base and cave level, 3) Pleistocene incision and karstification in association with glaciation, and 4) the particular case of karstified evaporites. In, gypsum and salt speleogenesis is characterized by rapid dissolution and subsidence. In European catchments, gypsum cave enlargement has occurred during cold climate periods, while limestone caves formed during warm interglacial or interstadial phases. However, in limestone rocks, the bulk of karstic cave fills correspond to cold periods, with thick, clastic sediments deposited under glacial conditions. Speleothems and tufa deposits are formed chiefly during interglacial periods. This demonstrates that, over Quaternary timescales, climate plays an important role in karst processes. The regional and local setting determines the modes of valley evolution and karstification, and the geomorphological framework plays a triggering factor to initiate speleogenesis.

In addition, our synthesis is used to propose four models of fluvial and karst evolution, from different settings: 1) in the Eastern Pyrenees, in limestone rocks, 2 and 3) in low elevation limestone plateaus of the Eastern Paris Basin, and 4) a rapidly-uplifted gypsum area in the Northern Apennines, Italy.

946 Future research should focus on improved reliability and application of dating methods,
947 because in many cases, numerical dating is not possible, due to a lack of alluvial sequences
948 such as fluvial terraces or sedimentary fills within karstic caves and surface depressions (such
949 as poljes and dolines). Even if alluvium is preserved in karstic terrain, it may not contain
950 sufficient siliceous content for OSL dating, or secondary carbonate concretions, such as
951 travertine or calcrete, for U-series dating. Moreover, U-series dating is further complicated by
952 the ingrowth of younger calcite into pre-existing sediments. Alluvial sequences might also bear
953 the imprint of sediment reworking, meaning that the sedimentary sequence is not indicative of
954 primary formation mechanisms. Further research should also include other karstic regions,
955 especially low latitude regions, as well as arid regions, around the Mediterranean Sea, to
956 enhance our understanding of karstic processes in other global regions.
957
958
959 **References**
960
961 Abel, T., Hinderer, M., Sauter, M., 2002. Karst genesis of the Swabian Alb, south
962 Germany,since the Pliocene. Acta Geologica Polonica, 52, 1, 43–54.
963 Adamson, K.R., Woodward, J.C., Hughes, P.D., 2014. Glaciers and rivers: Pleistocene
964 uncoupling in a Mediterranean mountain karst. Quaternary Science Reviews 94, 28–43.
965 Adamson, K., Candy, I., Whitfield, L., 2015. Coupled micromorphological and stable isotope
966 analysis of Quaternary calcrete development. Quaternary Research, 84 (2), 272-286.
967 Adamson, K. R., Woodward, J. C., Hughes, P. D. 2016a. Middle Pleistocene glacial outwash
968 in poljes of the Dinaric karst. *In:* Gao, Y. and Alexander Jr, E.C (Eds) Caves and Karst Across
969 Time. Geological Society of America, Vol. 516, 247–263.
970 Adamson, K.R., Woodward, J.C., Hughes, P.D., Giglio, F., Del Bianco, F., 2016b. Middle
971 Pleistocene glaciation, alluvial fan development and sea-level changes in the Bay of Kotor,
972 Montenegro. *In:* Hughes, P. D. and Woodward, J. C. (Eds) Quaternary Glaciation in the
973 Mediterranean Mountains Geological Society, London, Special Publications, 433, SP433-13.
974 Ambert, M. and Ambert P., 1995. Karstification des plateaux et encaissement des vallées au
975 cours du Néogène et du Quaternaire dans les Grands Causses méridionaux (Larzac, Blandas).
976 Géologie de la France, 4, 37–50.
977 Anthony, D.M., and Granger, D.E., 2007. A new chronology for the age of Appalachian
978 erosional surfaces determined by cosmogenic nuclides in cave sediments. Earth Surface
979 Processes and Landforms. Volume 32, Issue 6, 874–887.

980 Antoine, P., 1994. The Somme Valley terrace system (northern France): a model of river
981 response to Quaternary climatic variations since 800,000 BP. Terra Nova 6, 453–464.
982 Antoine, P., Lautridou, J.P, Laurent, M., 2000. Long-term fluvial archives in NW France:
983 response of the Seine and Somme rivers to tectonic movements, climatic variations and sea-
984 level changes. Geomorphology 33, 3-4,183–207.
985 Antoine, P., Limondin-Lozouet, N., Auguste, P., Locht, J.L., Galheb, B., Reyss, J.L., Escude,
986 E., Carbonel, P., Mercier, N., Bahain, J.J., Falguères, C., Voinchet, P., 2006. Le tuf de Caours
987 (Somme, France): mise en évidence d'une séquence éémienne et d'un site paléolithique associé.
988 Quaternaire 17,4, 281-320.
989 Audra, P., Ed., 2010, Grottes et karsts de France. Karstologia Mémoires, n° 19, 44–45.
990 Audra, P., 2010, La spéléogenèse épigène. *In:* Audra, P., Ed, 2010. Grottes et karsts de France.
991 Karstologia Mémoires, 19, 44–45.
992 Audra, P., Camus, H., Rochette, P., 2001. Le karst des plateaux jurassiques de la moyenne
993 vallée de l'Ardèche : datations par paléomagnétisme des phases d'évolution plio-quaternaire
994 (aven de la Combe Rajeau). Bull. Soc. Géol. France, 172, 1, 121–129.
995 Audra, P., Mocochain, L., Camus, H., Gilli, É., Clauzon, G., Bigot, J.-Y., 2004. The effect of
996 the Messinian Deep Stage on karst development around the Mediterranean Sea. Examples from
997 Southern France. Geodinamica Acta, 17, 6, 27–38.
998 Audra P., Bini A., Gabrovsek F., Häuselmann P., Hobléa F., Jeannin P.Y., Kunaver J.,
999 Monbaron M., Sustersic F., Tognini P., Trimmel H., Wilberger A., 2007. Cave and karst
1000 evolution in the Alps and their relation to paleoclimate and paleotopography. Acta Carsologica
1001 36-1, 53–67.
1002 Audra, P., Mocochain, L., Bigot, J.-Y., Nobécourt, J.-C., 2009. The association between bubble
1003 trails and folia: a morphological and sedimentary indicator of hypogenic speleogenesis by
1004 degassing, example from Adaouste Cave (Provence, France). International Journal of
1005 Speleology, Bologna, 38, 2: 93-102.
1006 Audra, P. and Palmer, A.N., 2011. The pattern of caves: controls of epigenic speleogenesis.
1007 Géomorphologie, 4, 359–378.
1008 Audra, P. and Palmer, A.N., 2013. The vertical dimension of karst: controls of vertical cave
1009 pattern. *In:* Shroder, J. (Editor in chief), Frumkin, A. (Ed.), Treatise on Geomorphology.
1010 Academic Press, San Diego, CA, 6, Karst Geomorphology, 186–206.
1011 Bastin, B. and Gewelt, M., 1986. Analyse pollinique et datation ^{14}C de concrétions
1012 stalagmitiques holocènes : apports complémentaires des deux méthodes. Géographie physique
1013 et Quaternaire, 40, 2, 185-196.

1014 Bazalgette, L. and Petit, J.P., 2005. Fold amplification and style transition involving fractured
1015 dip-domain boundaries; buckling experiments in brittle paraffin wax multilayers and
1016 comparison with natural examples. Geological Society Special Publications (2007) 270: 157-
1017 169.
1018 Benito, G., Pérez-González, A., Gutiérrez, F., Machado, M.J., 1998. River response to
1019 Quaternary subsidence due to evaporite solution (Gállego River, Ebro Basin, Spain).
1020 Geomorphology 22, 243–263.
1021 Benito, G., Sancho, C., Peña, J.L., Machado, M.J., Rhodes, E.J., 2010. Large-scale karst
1022 subsidence and accelerated fluvial aggradation during MIS6 in NE Spain: climatic and
1023 paleohydrological implications. Quaternary Science Reviews 29, 2694–2704.
1024 Bigot, J.-Y. and Audra, P., 2010. Les cavités parakarstiques des grès et des conglomérats. *In:*
1025 Audra, Ph., ed, 2010. Grottes et karsts de France. Karstologia Mémoires, 19, 84–85.
1026 Bridgland, D. and Westaway, R., 2007. Climatically controlled river terrace straircases: A
1027 wordwise Quaternary phenomenon. Geomorphology, 98, 285-315.
1028 Bridgland, D., Westaway, R., Cordier, S., 2009. Les causes de l'étagement des terrasses
1029 alluviales à travers le monde. Quaternaire, 20, 4, 5–23.
1030 Bruthans J. and Zeman O., 2003. Factors controlling exokarst morphology and sediment
1031 transport trough caves: comparison of carbonate and salt karst. Acta Carsologica 32-1, 83-99.
1032 Bruxelles, L., Astruc, J.-L., Simon-Coinçon, R., Ciszak, R., 2013. Histoire des paysages et
1033 Préhistoire : l'apport de la connaissance géomorphologique du Quercy pour la compréhension
1034 de l'environnement paléolithique. Actes de la session C67, XVème Congrès mondial de
1035 l'UISPP, Lisbonne, sept. 2006, PALEO, supplément 4, 21–36.
1036 Buffard, R. and Fischer, H., 1993. Les gisements de fer de la région de Kisanga (Shaba
1037 méridional, Zaïre), colmatages d'un paléokarst du Protérozoïque supérieur, Karstologia, 21, 51-
1038 55.
1039 Calaforra, J.M. and Pulido-Bosch, A., 2003. Evolution of the gypsum karst of Sorbas (SE
1040 Spain). Geomorphology, 50, 1, 173-180.
1041 Calvet, M., Gunnell, Y., Braucher, R., Hez, G., Bourlès, D., Guillouc, V., Delmas, M., ASTER
1042 Team, 2015. Cave levels as proxies for measuring post-orogenic uplift: Evidence from
1043 cosmogenic dating of alluvium-filled caves in the French Pyrenees, Geomorphology, 246, 617–
1044 633.
1045 Campy, M., 1982. Le Quaternaire franc-comtois. Essai chronologique et paléoclimatique.
1046 Thèse d'État, 575 p., Besançon.

Camus, H., 1997. Formations des réseaux karstiques et creusement des vallées : l'exemple du Larzac méridional, Hérault, France. Karstologia, 29, 1, 23–42.

Camus, H., 2010. L'aven de la Leïcasse, un modèle de spéléogenèse des Causses méridionaux. In: Audra, P., Ed, 2010. Grottes et karsts de France. Karstologia Mémoires, 19, 310–311.

Candy, I., Black, S., Sellwood, B.W., 2005. U-series isochron dating of immature and mature calcretes as a basis for constructing Quaternary landform chronologies for the Sorbas basin, southeast Spain. Quaternary Research, 64 (1), 100-111.

Clauzon, G., 1978. The Messinian Var canyon (Provence, Southern France). Paleogeographic implications. Marine Geology 27, 3-4, 231–246.

Columbu, A., De Waele, J., Forti, P., Montagna, P., Picotti, V., Pons-Branchu, E., Hellstrom, J., Bajo, P., Drysdale, R., 2015. Gypsum caves as indicators of climate-driven river incision and aggradation in a rapidly uplifting region. Geology, 43, 6, 539-542.

Cordier, S., Harmand, D., Frechen, M., Beiner, M., 2006: Fluvial system response to Middle and Upper Pleistocene climate change in the Meurthe and Moselle valleys (Eastern Paris Basin and Rhenish Massif). Quaternary Science Reviews, 25, 1460–1474.

Cordy, J.-M., Bastin, B., Demaret-Fairon, M., Ek, C., Geeraerts, R., Groessens-Van Dyck, M.C., Oze, A., Peuchot, R., Quinif, Y., Thorez, J., Ulrix-Closset, M., 1993. La grotte de la Belle-Roche (Sprimont, Province de Liège) : un gisement paléontologique et archéologique d'exception au Bénélux. Bull. de la Classe des sciences, Académie royale de Belgique, 1-6, 165–186.

Couchoud, I., 2008. Les spéléothèmes, archives des variations paléoenvironnementales. Quaternaire, 19, 4, 255–274.

Dabkowski, J., Limondin-Lozouet, N., Antoine, P., Marca-Bell, A., Andrews, J., 2011. Enregistrement des variations climatiques au cours des interglaciaires d'après l'étude des isotopes stables de la calcite de tufs calcaires pléistocènes du nord de la France : exemple des séquences de Caours (SIM 5e ; Somme) et de La Celle-Sur-Seine (SIM 11 ; Seine-et- Marne). Quaternaire, 22, (4), 275-283.

Dabkowski, J., Limondin-Lozouet, N., Anders, J., Marca-Bell, A., Antoine, P., 2016. Climatic and environmental variations during the Last Interglacial recorded in a Northern France Tufa (Caours, Somme Basin). Comparisons with regional to global records. Quaternaire, 27, (3), 249-261.

Delannoy, J.-J., 1982. Les variations spatio-temporelles de la corrosion karstique dans un massif de moyenne montagne : le Vercors. Revue de géographie alpine, 70, 3, 241-255.

1080 Delannoy, J.-J., 1997, Recherches géomorphologiques sur les massifs karstiques du Vercors et
1081 de la transversale de Ronda (Andalousie). Les apports morphogéniques du karst. Thèse de
1082 doctorat d'état en géographie / Université Joseph Fourier / Grenoble 1, 706 p.
1083 Delannoy, J.-J., Perrette, Y., Destombes, J.-L., Peiry, J.-L., 1999. Excursion 4 : le Vercors.
1084 Itinéraire : Ste Eulalie-en-Royans - Grands Goulets - Val médian - Gorges de la Bourne -
1085 Grottes de Choranche. Cahiers savoisiens de Géographie, [field excursions guide of the
1086 European Conference "Karst 99", Grands Causses - Vercors, 10-15 September 1999],
1087 Université de Savoie: 75-108.
1088 Devos, A., Lejeune, O., Chopin, E., 2007. Structural control on surface flow in karstic
1089 environnement, Geodinamica Acta, 20/6, 393–402.
1090 Devos, A., Sosson, C., Fronteau, G., Lejeune, O., 2009. Les tuffières de Vormy et des
1091 Fontinettes (Aisne, Marne, France): marqueurs de la faible karstification des calcaires lutétiens
1092 de l'Est du Bassin parisien? Karstologia 54, 37–48.
1093 Devos, A., Chalumeau, Sosson, C., Fronteau, G., Turmel, A., Lejeune, O., 2011: La
1094 fantômisation des calcaires lutétiens du bassin de Paris – Apport des carrières souterraines,
1095 Karstologia 58, 15–28.
1096 Devos, A., Bollot, N., Chalumeau, L., Fronteau, G., Lejeune, O., 2015. Impact of lateral
1097 variations of geologic facies on water resources in homogeneous basins - Example of tertiary
1098 plateaus in the Paris Basin. Geodinamica acta, 27, 1, 15–24.
1099 Dunai, T., 2010. Cosmogenic nuclides - Principles, Concepts and Applications in the Earth
1100 Surface Sciences, Cambridge University Press, 187 p.
1101 Ek, C., 1961. Conduits souterrains en relation avec les terrasses fluviales. Annales de la Société
1102 géologique de Belgique, Liège, t. LXXXIV, 313–340.
1103 Fairchild, I. J. and Baker, A., 2012. Speleothem Science: From Process to Past Environments,
1104 Wiley-Blackwell, 450 p.
1105 Ford, D.C. and Ewers, R.O., 1978. The development of limestone cave systems in the
1106 dimensions of length and depth. International Journal of Speleology, 10, 213–244.
1107 Ford, D. and Williams, P., 1989. Karst geomorphology and hydrology, Unwin Hyman, 601 p.
1108 Frank, N., Kober, B., Mangini, A., 2006. Carbonate precipitation, U-series dating and U-
1109 isotopic variations in a Holocene travertine platform at Bad Langensalza - Thuringia Basin,
1110 Germany. *In:* Tufs calcaires et travertins quaternaires: morphogenèse, biocénoses, paléoclimats
1111 et implantations paléolithiques. 2ème partie. Quaternaire, 17, 4, 333–342.
1112 Gabrovšek, F., Häuselmann, P., Audra, P., 2014. 'Looping caves' versus 'water table caves':
1113 the role of base-level changes and recharge variations in cave development. Geomorphology

204, 683–691.
Gázquez, F., Calaforra, J.M., Evans, N.P., Hodell, D.A., 2016. Using stable isotopes (δ18O and δD) of gypsum hydration water to unravel the mode of gypsum speleothem formation in semi-arid caves. EGU General Assembly 2016, held 17-22 April, 2016 in Vienna Austria, p.8911.
Gilli, E., 2010. Les grands volumes karstiques souterrains. *In:* Audra, P., Ed, Grottes et karsts de France. Karstologia Mémoires, 19, 54-55.
Granger, D.E., 2014. Cosmogenic Nuclide Burial Dating in Archaeology and Paleoanthropology. *In:* Treatise on Geochemistry: Second Edition. Elsevier Ltd, 81–97.
Granger, D.E., Kirchner, J.W., Finkel, R.C., 1997. Quaternary downcutting rate of the New River, Virginia, measured from differential decay of cosmogenic 26Al and 10Be in cave-deposited alluvium. Geology, 25, 2, 107–110.
Granger, D.E., Fabel, D., Palmer, A.N., 2001. Pliocene–Pleistocene incision of the Green River, Kentucky, determined from radioactive decay of cosmogenic ^{26}Al and ^{10}Be in Mammoth Cave sediments: Geological Society of America Bulletin, 113, 825–836.
Granger, D.E. and Muzikar, P.F., 2001. Dating sediment burial with in situ-produced cosmogenic nuclides: theory, techniques, and limitations. Earth Planet. Sci. Lett. 188, 269–281.
Guifang, Y., Xujiao Zh., Mingzhong T., Yamin P., Anze C., Zhiliang G., Zhiyun N., Zhen Y., 2011. Geomorphological and sedimentological comparison of fluvial terraces and karst caves in Zhangjiajie, northwest Hunan, China: an archive of sandstone landform development. Environ Earth Sci, 64, 671–683.
Habib, B., 2015. Relations entre karstification, cadre morphostructural et incisions des vallées dans les calcaires du Dogger en Haute-Saône (plateaux de Vesoul et de Combeaufontaine). Thèse de doctorat, Université de Lorraine, 460 p.
Harmand, D., Lejeune, O., Jaillet, S., Allouc, J., Occhietti, S., Brulhet, J., Devos, A., Fauvel, P.-J., Hamelin, B., Laurain, M., Le Roux, J., Marre, A., Pons-Branchu, E., Quinif, Y., 2004. Dynamique de l'érosion dans le Barrois et le Perthois: incision et karstification dans les bassins-versants de la Marne, la Saulx et l'Ornain. Quaternaire, 15, 4, 305–318.
Harmand, D. and Cordier, S., 2012. The Pleistocene terrace staircases of the present and past rivers downstream from the Vosges Massif (Meuse and Moselle catchments). Netherlands Journal of geosciences-Geologie en Mijnbouw, 91-1/2, 91–109.
Harvey, A.M., Whitfield, E., Stokes, M. & Mather, A.E. 2014. The late Neogene to Quaternary drainage evolution of the uplifted Neogene Sedimentary Basins of Almeria, Betic Chain. Landscapes and Landforms of Spain, 37-61.

1147 Häuselmann, P., 2002. Cave genesis and its relationship to surface processes: Investigations in
1148 the Siebenhengste region (BE, Switzerland). - PhD thesis, Université de Fribourg, 168 p.
1149 Häuselmann, P. and Granger, D.E., 2005. Dating of caves by cosmogenic nuclides: method,
1150 possibilities, and the Siebenhengste example (Switzerland). Acta Carsologica, 34/1, 3, 43–50.
1151 Häuselmann, P., Granger, D.E., Jeannin P.Y., Lauritzen S.E., 2007. Abrupt glacial valley
1152 incision at 0.8 Ma dated from caves deposits in Switzerland, Geology, 35, 2, 143-146.
1153 Häuselmann, P., Mihevc, A., Pruner, P., Horáček, I., Čermák, S., Hercman, H., Sahy, D., Fiebig,
1154 M., Hajna, N.Z., Bosák, P., 2015. Snežna jama (Slovenia): Interdisciplinary dating of cave
1155 sediments and implication for landscape evolution. Geomorphology, 247, 10–24.
1156 Hez, G., Jaillet, S., Calvet, M., Delannoy, J.-J, 2015. Un enregistreur exceptionnel de l'incision
1157 de la vallée de la Têt : Le karst de Villefranche. Pyrénées-Orientales – France. Kartologia n°
1158 65, *in press*.
1159 Hill, C.A., 1987. Geology of Carlsbad Cavern and other caves in the Guadalupe Mountains,
1160 New Mexico and Texas. New Mexico Bureau of Mines and Mineral Resources. Bulletin 117,
1161 150 p.
1162 Hobléa, F., Jaillet, S., Maire, R., 2001. Erosion et ruissellement sur karst nu en contexte
1163 subpolaire océanique : les îles calcaires de Patagonie (Magallanes, Chili). Karstologia, 38, 2,
1164 13-18.
1165 Hobléa, F., Häuselmann, P., Kubik, P., 2011. Cosmogenic nuclide dating of cave deposits of
1166 Mount Granier (Hauts de Chartreuse Nature Reserve, France): morphogenic and
1167 palaeogeographical implications. Géomorphologie: relief, processus, environnement 4, 395–
1168 406.
1169 Hoke, G. D., Liu-Zeng, J., Hren, M. T., Wissink, G. K., and Garzione, C. N., 2014. Stable
1170 isotopes reveal high southeast Tibetan Plateau margin since the Paleogene. Earth and Planetary
1171 Science Letters, 394, 270-278.
1172 Hughes, P. D., Woodward, J. C. and Gibbard, P. L. (2006). Quaternary glacial history of the
1173 Mediterranean mountains. Progress in Physical Geography, 30(3), 334-364.
1174 Hughes, P. D., Woodward, J. C., van Calsteren, P. C., Thomas, L. E., Adamson, K. R., 2010,
1175 Pleistocene ice caps on the coastal mountains of the Adriatic Sea. Quaternary Science Reviews,
1176 29 (27-28), 3690–3708.
1177 Hughes, P.D., Woodward, J.C., Van Calsteren, P.C. and Thomas, L.E., 2011. The glacial
1178 history of the Dinaric Alps, Montenegro. Quaternary Science Reviews, 30(23), 3393-3412.
1179 Huxtable, J., Aitken, M. J., 1991. Thermoluminescence dating: results for the late Pleistocene.
1180 In: Raynal, J.-P., Miallier, D. (éd.). Datation et caractérisation des milieux pléistocènes. Cah.

1181 Quat., CNRS, Paris (actes des symposiums 11 et 17 de la 11ème réunion des Sciences de la
1182 Terre, Clermont-Ferrand, 25-27 mars 1986), 16, 19-24.
1183 Jaillet, S., 2000. Un karst couvert de bas-plateau : le Barrois (Lorraine / Champagne, France).
1184 Structure - Fonctionnement - Evolution. Thèse de doctorat, Université de Bordeaux III, 2 vol.,
1185 712 p.
1186 Jaillet, S., Pons-branchu, E., Brulhet, J., Hamelin, B., 2004. Karstification as a
1187 geomorphological witness of river incision: example of the Marne Valley and Cousance karst
1188 system (Eastern Paris Bassin). Terra Nova, 16, 4, 167–172.
1189 Kukla, G., 2005. Saalian supercycle, Mindel/Riss Interglacial and Milankovitch's dating.
1190 Quaternary Science Reviews, 24, 14–15, 1573–1583.
1191 Le Roux, J. and Harmand, D., 1998. Contrôle morphostructural de l'histoire d'un réseau
1192 hydrographique : le site de la capture de la Moselle. Geodinamica acta, 11, 4, 149-162.
1193 Le Roux, J. and Harmand, D., 2003. Origin of the hydrographic network in the Eastern Paris
1194 Basin and its border massifs. Hypothesis, Structural, Morphologic and Hydrologic
1195 consequences. Special conference on paleoweathering and paleosurfaces in the Ardenne-Eifel
1196 region at Preizerdaul (Luxembourg) on 14 to 17 may 2003, Quesnel, coordinator, Géologie de
1197 la France, 1, 4, 105-110.
1198 Lewin, J. and Gibbard, P.L., 2010. Quaternary river terraces in England: Forms, sediments and
1199 processes. Geomorphology 120, 293-311.
1200 Lewin, J. and Woodward, J., 2009. Karst Geomorphology and Environnemental Change
1201 (chapter 10). *In:* Woodward, J. Ed., 2009. The Physical Geography of the Mediterranean.
1202 Oxford University Press, 287-317.
1203 Limondin-Lozouet, N., Antoine, P., Auguste, P., Bahain, J.-J., Carbonel, P., Chaussé, Ch.,
1204 Connet, N., Dupéron, J., Dupéron, M., Falguères, Ch., Freytet, P., Ghaleb, B., Jolly-Saad, M.-
1205 C., Lhomme, V., Pierre Lozouet, P., Mercier, N., Pastre, J.-F., Voinchet, P., 2006. Le tuf
1206 calcaire de La Celle-sur-Seine (Seine et Marne) : nouvelles données sur un site clé du stade 11
1207 dans le Nord de la France. Quaternaire, 17, 2, 5–29.
1208 Liu, Y., Wang, S.J., Xu, S., Liu, X.M., Fabel, D., Zhang, X.B., Luo, W.J., Cheng, A.Y., 2013.
1209 New evidence for the incision history of the Liuchong River, Southwest China, from
1210 cosmogenic $^{26}Al/^{10}Be$ burial ages in cave sediments. J. Asian Earth Sci., 73, 274–283.
1211 Losson, B., 2003. Karstification et capture de la Moselle (Lorraine, France) : vers une
1212 identification des interactions. Thèse de Géographie physique. Université de Metz. Vol. 1
1213 (texte) : 510 p, Vol. des planches : 89 pl., Vol. des annexes, 227 p.

Losson, B., Corbonnois, J., Argant, J., Brulhet, J., Pons-Branchu, E., Quinif, Y., 2006. Interprétation paléoclimatique des remplissages endokarstiques de la vallée de la Moselle à Pierre-la-Treiche (Lorraine, France). Géomorphologie : relief, processus, environnement, 1, 37–48.

Lucha, P., Gutiérrez, F., Pedro Galve, J., Guerrero, J., 2012. Geomorphic and stratigraphic evidence of incision-induced halokinetic uplift and dissolution subsidence in transverse drainages crossing the evaporite-cored Barbastro–Balaguer Anticline (Ebro Basin, NE Spain). Geomorphology, 171–172, 154–172.

Mangin, A., 1975. Contribution à l'étude hydrodynamique des aquifères karstiques. Annales de spéléologie, 29, n° 3, 283–332 ; 29, n° 4, 495–601 ; 30, n° 1, 21–124. Thèse d'état, Dijon.

Mather, A.E., 2000. Adjustment of a drainage network to capture induced base-level change: an example from the Sorbas Basin, SE Spain. Geomorphology, 34, 3-4, 271-289.

McPhillips, D., Hoke, G. D., Liu-Zeng, J., Bierman, P. R., Rood, D. H., Niedermann, S., 2016. Dating the incision of the Yangtze River gorge at the First Bend using three-nuclide burial ages, Geophys. Res. Lett., 43, 101–110.

Mocochain, L., Clauzon, G., Bigot, J.-Y., 2006. Réponses de l'endokarst ardéchois aux variations eustatiques générées par la crise de salinité messinienne. Bulletin de la Société géologique de France, Paris, 177, 1, 27-36.

Mocochain, L., Audra, P., Clauzon, G., Bellier., O., Bigot, J.-Y., Monteil, Ph., 2009. The effect of river dynamics induced by the Messinian Salinity Crisis on karst landscape and caves: example of the Lower Ardèche River (and Rhône valley). Geomorphology, 106, 46–61.

Moreno, D., Falguères, Ch., Pérez-González, A., Duval, M., Voinchet, P., Benito-Calvo, A., Ortega, A. I., Bahain, J.-J., Sala, R., Carbonell, E., Bermúdez de Castro, J. M., Arsuaga, J.L., 2012. ESR chronology of alluvial deposits in the Arlanzón valley (Atapuerca, Spain): Contemporaneity with Atapuerca Gran Dolina site. Quaternary Geochronology, 10, 418–423.

Nicod, J., 2010. Les étapes de la karstologie en France. *In:* Audra, P., Ed, 2010. Grottes et karsts de France. Karstologia Mémoires, 19, 16–17.

Ortega, A.I., Benito-Calvo, A., Pérez-González, A., Martín-Merino, M.A., Pérez-Martínez, R., Parés, J.M., Aramburu, A., Arsuaga, J.L., Bermúdez de Castro, J.M., Carbonell, E., 2013. Evolution of multilevel caves in the Sierra de Atapuerca (Burgos, Spain) and its relations to human occupation. Geomorphology, 196, 122–137.

Osborne, R. A. L., 2007. The world's oldest caves: how did they survive and what can they tell us? Acta carsologica, 36, 133–142.

Palmer, A.N., 1991. Origin and morphology of limestone caves. Geological Society of America Bulletin 103, 1-21.

Palmer, A.N, 2007. Cave geology. Cave books, 454 p.

Palmer, A.N. and Palmer, M.V., 1993, Geologic leveling survey in Logsdon River, Mammoth Cave: Cave Research Foundation Annual Report 1992, 32–34.

Piccini, L., 2011. Speleogenesis in highly geodynamic contexts: The quaternary evolution of Monte Corchia multi-level karst system (Alpi Apuane, Italy). Geomorphology, 134, 49–61.

Pons-Branchu E., Hamelin B., Losson B., Jaillet S., Brulhet J., 2010. Speleothem evidence of warm episodes in northeast France during Marine Oxygen Isotope Stage 3 and implications for permafrost distribution in northern Europe. Quaternary Research, 2010, 74 (2), p. 246-251.

Quinif, Y., 1989. La notion d'étages de grottes dans le karst belge. Karstologia, 13, 41–49.

Quinif, Y., 1999. Karst et évolution des rivières : le cas de l'Ardenne. Geodinamica Acta, Elsevier, Paris, 12, 3-4, 267-277.

Quinif, Y., 2006. Complex stratigraphic sequences in Belgian caves: correlation with climatic changes during the middle, the upper Pleistocene, and the Holocene. Geologica Belgica [En ligne], number 3-4 - Han-sur-Lesse Symposium - nov. 2004, 9, 231-244.

Quinif, Y., 2010. Fantômes de roche et fantômisation. Essai sur un nouveau paradigme en karstogenèse. Karstologia Mémoires, 18, 196 p.

Quinif, Y. and Maire, R., 1998. Pleistocene deposits in Pierre-Saint-Martin cave, French Pyrenees. Quaternary Research, 49, 37–50.

Richard, M., C. Falguères, Pons-Branchu, E., Bahain, J.-J., Voinchet, P., Lebon, M., Valladas, H., Dolo, J.-M., Puaud, S., Rué, M., Daujeard, C., Moncel, M.-H., Raynal, J.-P., 2015. Contribution of ESR/U-series dating to the chronology of late Middle Palaeolithic sites in the middle Rhône valley, Southeastern France. Quaternary Geochronology 30, 529–534.

Rixhon, G. & Demoulin, A. 2010. Fluvial terraces of the Amblève: a marker of the Quaternary river incision in the NE Ardenne massif (western Europe). Zeitschrift für Geomorphologie 54, 161–180.

Rixhon, G., Braucher, R., Bourlès, D., Siame, L., Bovy, B., Demoulin, A., 2011. Quaternary river incision in NE Ardennes (Belgium) – insights from $^{10}Be/^{26}Al$ dating of river terraces. Quat. Geochronol. 6, 273–284.

Rixhon, G., Bourlès, D.L., Braucher, R., Siame, L., Cordy, J.-M., & Demoulin, A., 2014. ^{10}Be dating of the Main Terrace level in the Amblève valley (Ardennes, Belgium): new age constraint on the archaeological and palaeontological filling of the Belle-Roche palaeokarst. Boreas, 43, 2, 528–542.

1281 Rixhon, G., Briant, R.M., Cordier, S., Duval, M., Jones, A., Scholz, D., 2016 (in press).
1282 Revealing the pace of river landscape evolution during the Quaternary: recent developments in
1283 numerical dating methods. Quaternary Science Reviews.
1284 Rodet, J., 1992. La craie et ses karsts. Centre normand d'étude du karst et des cavités du sous-
1285 sol et Groupe Seine, Rouen, 560 p.
1286 Rodet, J., 2013. Karst et évolution géomorphologique de la côte crayeuse à falaises de la
1287 Manche. L'exemple du Massif d'Aval (Etretat, Normandie, France). Quaternaire, Paris, 24, 3,
1288 303-314.
1289 Rohling, E. J., Grant, K., Bolshaw, M., Roberts, A. P., Siddall, M., Hemleben, Ch., Kucera, M.,
1290 2009. Antarctic temperature and global sea level closely coupled over the past five glacial
1291 cycles. Nature Geoscience 2, 500 – 504.
1292 Seranne, M., Camus, H., Lucazeau, F., Barbarand, J., Quinif, Y., 2002. Surrection et érosion
1293 polyphasées de la Bordure cévenole. Un exemple de morphogenèse lente. Bulletin Société
1294 Géologique de France, 173, 2, 97–112.
1295 Stepišnik, U., Ferk, M., Kodelja, B., Medenjak, G., Mihevc, A., Natek, K., Žebre, M., 2009.
1296 Glaciokarst of western Orjen, Montenegro. Cave and Karst Science 36 (1), 21-28.
1297 Stock, G.M., Anderson, R.S., Finkel, R.C., 2004. Pace of landscape evolution in the Sierra
1298 Nevada, California, revealed by cosmogenic dating of cave sediments. Geology, 32, 193-196.
1299 Stock, G.M., Anderson, R.S., Finkel, R.C., 2005. Rates of erosion and topographic evolution
1300 of the Sierra Nevada, California, inferred from cosmogenic 26Al and 10Be concentrations.
1301 Earth Surf. Process. Landforms, 30, 985–1006.
1302 Stokes, M., Mather, A. E., Harvey, A. M., 2002. Quantification of river-capture-induced base-
1303 level changes and landscape development, Sorbas Basin, SE Spain. Geological Society,
1304 London, Special Publications 191, 23-35.
1305 Tassy, A., Mocochain, L., Bellier, O., Braucher, R., Gattacceca, J., Bourlès, D., 2013. Coupling
1306 cosmogenic dating and magnetostratigraphy to constrain the chronological evolution of peri-
1307 Mediterranean karsts during the Messinian and the Pliocene: Example of Ardèche Valley,
1308 Southern France. Geomorphology, 189, 81–92.
1309 Tassy, A., Fournier, F., Munch, P., Borgomano, J., Thinon, I., Fabri, M.-C., Rabineau, M.,
1310 Arfib, B., Begot, J., Beslier, M.-O., Cornée, J.-J., Fournillon, A., Gorini, C., Guennoc, P.,
1311 Léonide, P., Oudet, J., Paquet, F., Sage, F., Toullec, R., 2014. Discovery of Messinian canyons
1312 and new seismic stratigraphic model, offshore Provence (SE France): Implications for the
1313 hydrographic network reconstruction. Marine and Petroleum Geology, 57, 25–50.

1314 Tognini, P., 1999. The Mt. Bisbino (Northern Italy) karst: a new speleogenetic process. Etudes
1315 de géographie physique, supplément n° XXVIII [proceedings of the European Conference "
1316 Karst 99 ", Grands Causses - Vercors, 10-15 September 1999], CAGEP, Université de
1317 Provence, 185-190.
1318 Vergari, A. and Quinif, Y., 1997. Les paléokarsts du Hainaut (Belgique). Geodinamica Acta,
1319 10, 4, 175–187.
1320 Vernet, J.-L., Mercier, N., Bazile F., Brugal, J.-P., 2008. Travertins et terrasses de la moyenne
1321 vallée du Tarn à Millau (sud du Massif central, Aveyron, France) : datations OSL, contribution
1322 à la chronologie et aux paléoenvironnements. Quaternaire, 19, 1, 3–10.
1323 Wagner, T., Fabel, D., Fiebig, M., Häuselmann, P., Sahy, P., Sheng Xu, Kurt Stüwe, 2010.
1324 Young uplift in the non-glaciated parts of the Eastern Alps. Earth and Planetary Science Letters
1325 295, 159–169.
1326 Waltham, A.C., Simms, M.J., Farrant, A.R. & Goldie, H.S., 1997, Karst and Caves of Great
1327 Britain, Geological Conservation Review. Series, No. 12, Chapman and Hall, London, 358 p.
1328 Wang, F., Li, H., Zhu, R., Qin, F., 2004. Late Quaternary downcutting rates of the Qianyou
1329 River from U/Th speleothem dates, Qinling mountains, China. Quat. Research, 62, 194– 200.
1330 Webb, J.A., Fabel, D., Finlayson, B. L., Ellaway, M., Shu,L., Spiertz, H.-P., 1992. Denudation
1331 chronology from cave and river terrace levels: the case of the Buchan Karst, southeastern
1332 Australia. Geol. Mag. 129, 3, 307–317.
1333 White, W. B., 1988. Geomorphology and hydrology of karst terrains. Oxford University press,
1334 464 p.
1335 Whittaker, A. C., Boulton, S. J. (2012). Tectonic and climatic controls on knickpoint retreat
1336 rates and landscape response times, J. Geophys. Res., 117, F02024.
1337 Woodward, J.C., Hamlin, R. H. B., Macklin, M. G., Hughes, P. D., and Lewin, J., 2008. Glacial
1338 activity and catchment dynamics in northwest Greece: Long-term river behaviour and the
1339 slackwater sediment record for the last glacial to interglacial transition. Geomorphology, 101,1-
1340 2: 44–67.
1341
1342
1343 **Figures**
1344 Figure 1: Location map of the karstic areas discussed in the text.
1345 Figure 2: Schematic diagrams of the relationships between valley evolution and karstification:
1346 A) The concept of correlation between surface features (alluvial terraces) and subsurface
1347 karstification levels (caves) (modified from Abel *et al.,* 2002); B) Different types of cave profile

development, constrained by recharge (a and b) and base-level controls (c and d) (after Audra & Palmer, 2011).

Figure 3: Typology of the relationships between karst and valley incision, demonstrating the type of speleogenesis, characteristic morphologies, and examples (after Losson, unpublished)

Figure 4: Karst and entrenched valleys in the Eastern Paris Basin: A) Typology of the relations between karstification and valley evolution; B) hydraulic gradient between aquifer compartments and rivers (after Devos, unpublished).

Figure 5: Idealised models of *per descensum* (A) and *per ascensum* (B) speleogenesis using examples from the Vercors Subalpine Chain (A) and the Lower Ardèche River (B).

Figure 6: Two conceptual models of gypsum karst: A: interstratal karstification with contemporary underground erosion processes (after Calaforra & Pulido-Bosch, 2003); B: karst subsidence and accelerated fluvial aggradation (after Benito *et al.,* 2010)

Figure 7: A conceptual model of valley scale karstic and fluvial development in relation to river terrace records: A) successive stages of evolution of a karstic drain and a valley floor, B) schematic cross-section of relationships between cave passage and valley terrace during phase 4 (upstream part); C) Model elevation / time of the hydrographic network and the cave passage (Jaillet, unpublished)

Figure 8: Valley entrenchment during a Pleistocene glacial-interglacial cycle in limestone areas. A: connected cave and base levels of a same valley (plateau karst); B) speleogenesis in connection with an neighbouring valley (valley karst) (after Antoine, 1994; Losson, 2003; Antoine *et al.,* 2006; Quinif, 2006)

Figure 9: Conceptual model of climate-driven speleogenesis of gypsum cave systems in relation with valley incision and aggradation in moderately and rapid uptlifted gypsum area: A) climate-driven speleogenesis of epigenic gypsum cave systems, B) evolution of river valleys and adjacent gypsum cave systems (based on the Northern Apennines after Colombu *et al.,* 2015)

1381 **Figure 1**

1382

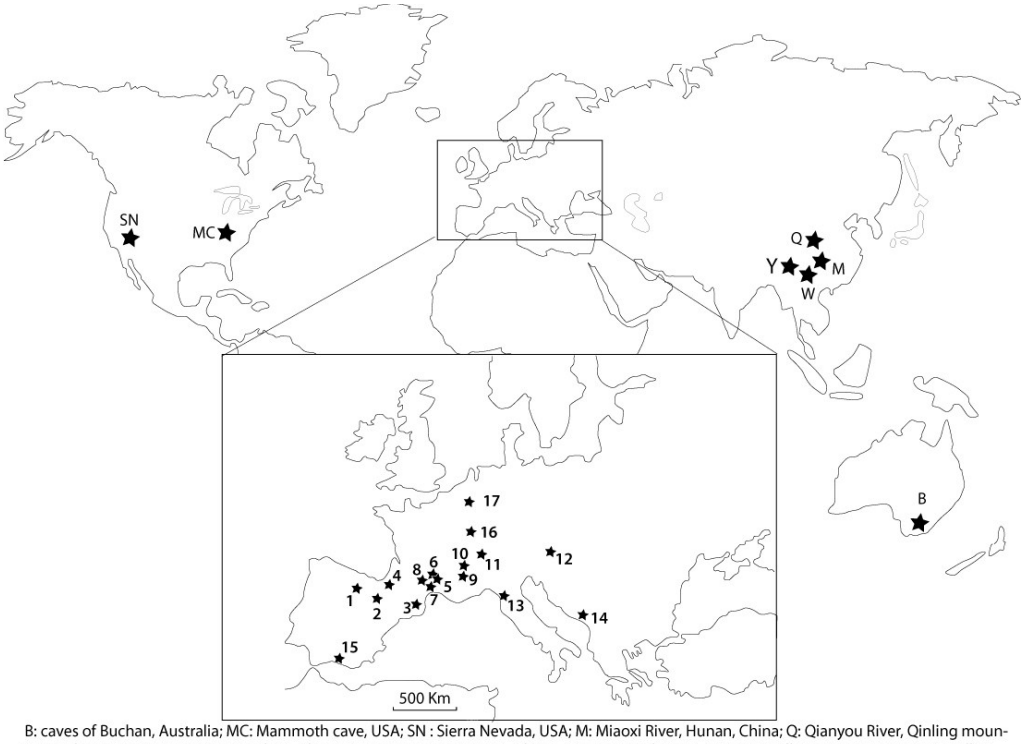

B: caves of Buchan, Australia; MC: Mammoth cave, USA; SN : Sierra Nevada, USA; M: Miaoxi River, Hunan, China; Q: Qianyou River, Qinling mountains, China; W: Wujiang River, Guizhou, China; Y: Yangzi Gorge,Yunnan, China; Europe: 1: Arlanzón, Spain; 2: Gállego River, Spain; 3: Têt valley, Eastern Pyrenees, France; 4: Pierre-Saint-Martin, Western Pyrenees, France; 5: Lower Ardèche valley, France; 6: Middle Ardèche valley, France; 7: Southern Larzac plateau, Grands Causses, France; 8: Tarn valley at Millau, Grands Causses, France; 9: Vercors, subalpine massif, France; 10: Mont Granier, Grande Chartreuse, subalpine massif, France; 11: Siebenhengste, Switzerland; 12: Mur valley, Eastern Alps, Austria; 13: Monte Corcia, Alpi Apuane, Italy; 14: Mount Orjen, Montenegro; 15: Gypsum karst of Sorbas, Spain; 16: Caves of Pierre-la-Treiche, Eastern Paris Basin, France; 17: Cave of Belle-Roche, Ardenne massif, Belgium

1383

1384

1385

Figure 2

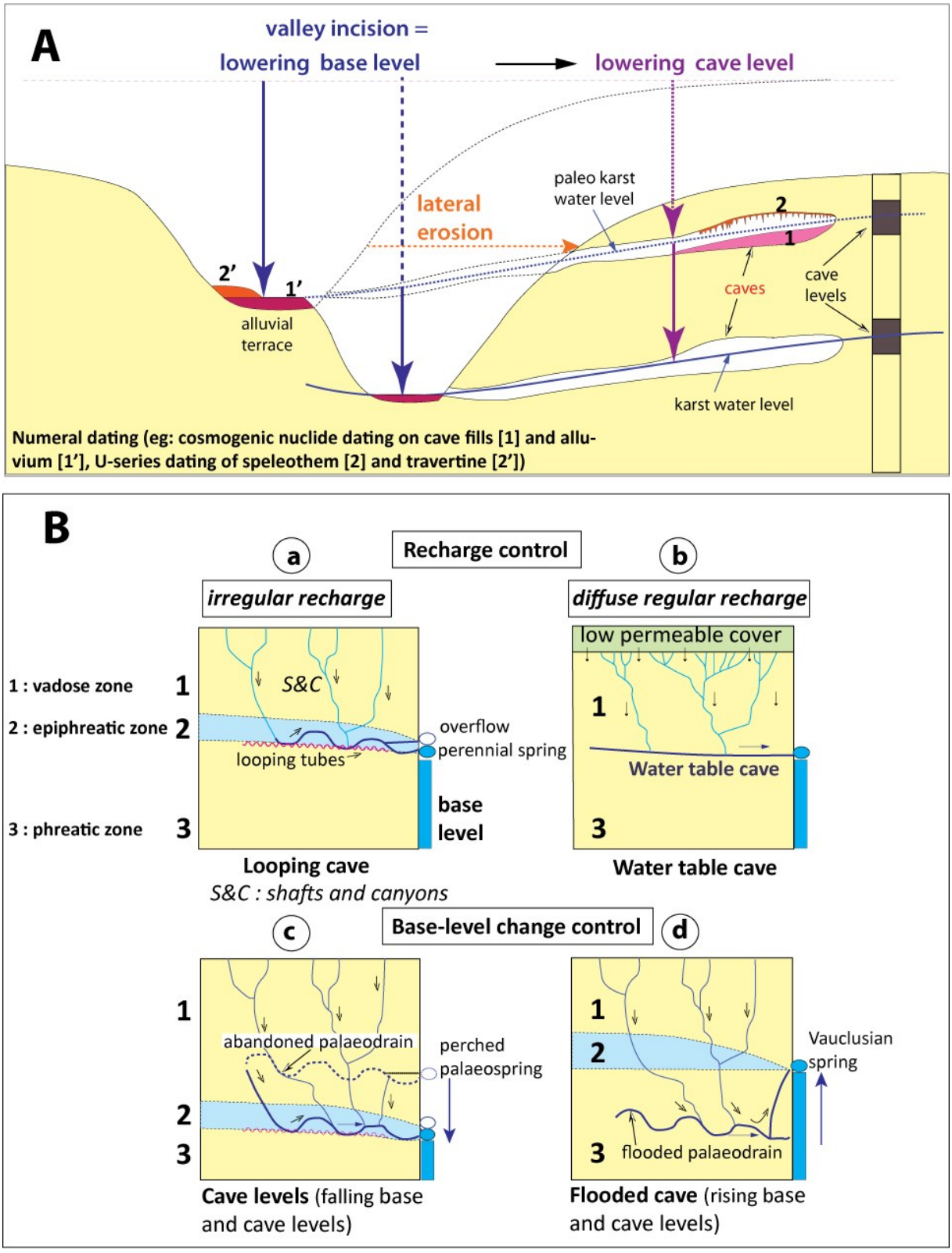
A
valley incision =
lowering base level
lowering cave level
paleo karst
water level
lateral
erosion
2
1
2'
1'
alluvial
terrace
caves
cave
levels
karst water level
Numeral dating (eg: cosmogenic nuclide dating on cave fills [1] and alluvium [1'], U-series dating of speleothem [2] and travertine [2'])
B
a
Recharge control
b
irregular recharge
diffuse regular recharge
low permeable cover
1 : vadose zone
2 : epiphreatic zone
3 : phreatic zone
S&C
looping tubes
overflow
perennial spring
base
level
Water table cave
Looping cave
Water table cave
S&C : shafts and canyons
c
Base-level change control
d
abandoned palaeodrain
perched
palaeospring
Vauclusian
spring
flooded palaeodrain
Cave levels (falling base and cave levels)
Flooded cave (rising base and cave levels)

Figure 3

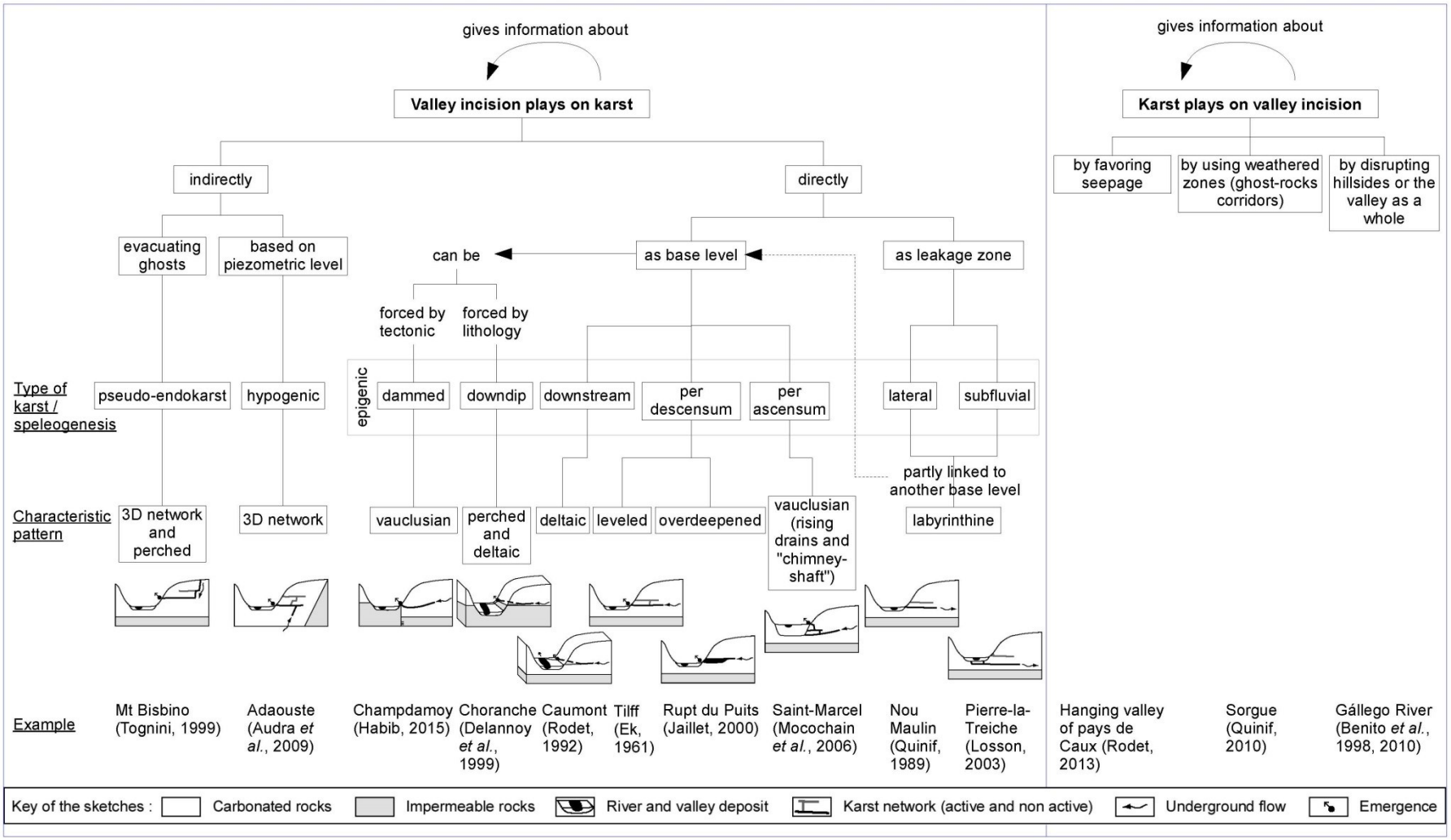
gives information about
Valley incision plays on karst
indirectly
directly
evacuating ghosts
based on piezometric level
can be
as base level
as leakage zone
forced by tectonic
forced by lithology
Type of karst / speleogenesis
pseudo-endokarst
hypogenic
epigenic
dammed
downdip
downstream
per descensum
per ascensum
lateral
subfluvial
partly linked to another base level
Characteristic pattern
3D network and perched
3D network
vauclusian
perched and deltaic
deltaic
leveled
overdeepened
vauclusian (rising drains and "chimney-shaft")
labyrinthine
Example
Mt Bisbino (Tognini, 1999)
Adaouste (Audra et al., 2009)
Champdamoy (Habib, 2015)
Choranche (Delannoy et al., 1999)
Caumont (Rodet, 1992)
Tilff (Ek, 1961)
Rupt du Puits (Jaillet, 2000)
Saint-Marcel (Mocochain et al., 2006)
Nou Maulin (Quinif, 1989)
Pierre-la-Treiche (Losson, 2003)
gives information about
Karst plays on valley incision
by favoring seepage
by using weathered zones (ghost-rocks corridors)
by disrupting hillsides or the valley as a whole
Hanging valley of pays de Caux (Rodet, 2013)
Sorgue (Quinif, 2010)
Gállego River (Benito et al., 1998, 2010)
Key of the sketches :
Carbonated rocks
Impermeable rocks
River and valley deposit
Karst network (active and non active)
Underground flow
Emergence

Figure 4

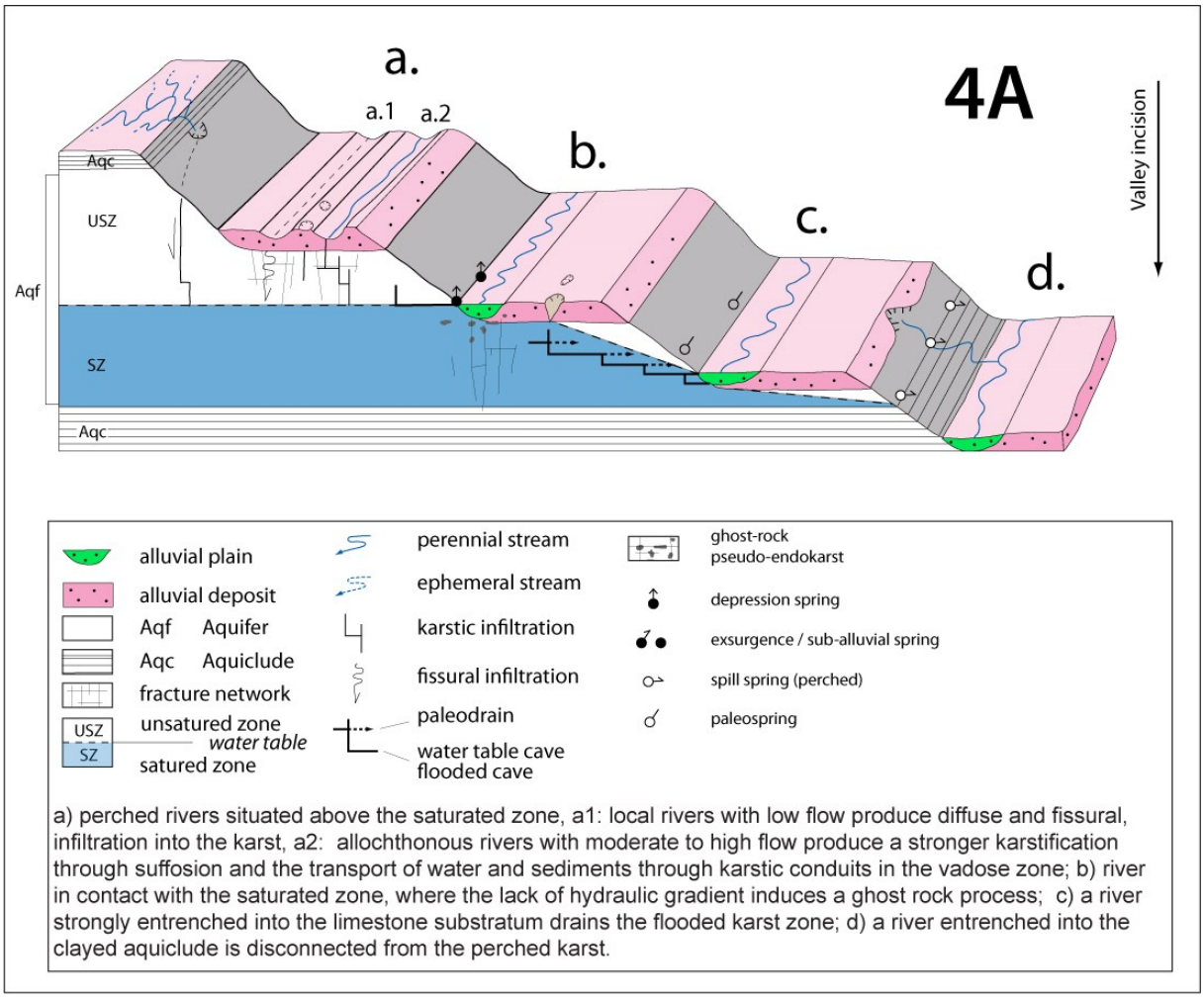

a) perched rivers situated above the saturated zone, a1: local rivers with low flow produce diffuse and fissural, infiltration into the karst, a2: allochthonous rivers with moderate to high flow produce a stronger karstification through suffosion and the transport of water and sediments through karstic conduits in the vadose zone; b) river in contact with the saturated zone, where the lack of hydraulic gradient induces a ghost rock process; c) a river strongly entrenched into the limestone substratum drains the flooded karst zone; d) a river entrenched into the clayed aquiclude is disconnected from the perched karst.

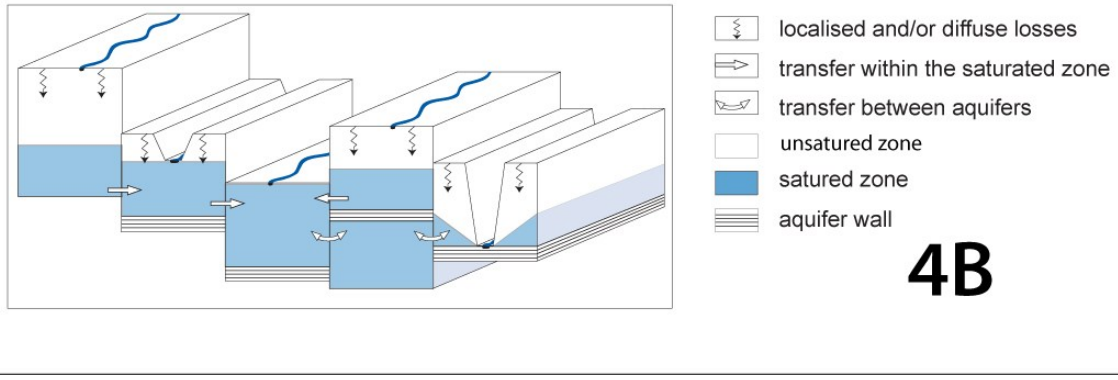

Figure 5

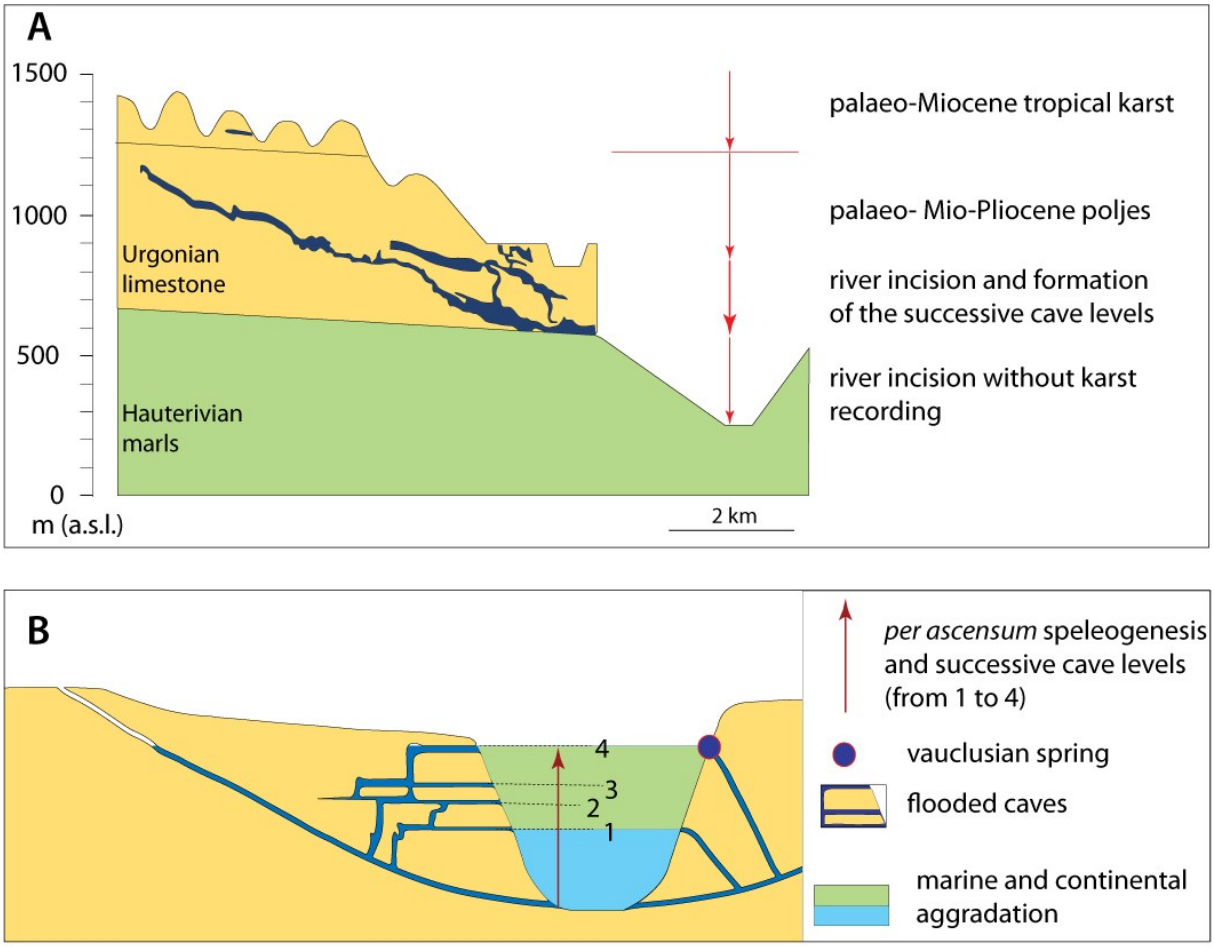

A: Per descensum speleogenesis incision in connection with uplift and valley incision (model of the Vercors subalpin chain, after Delannoy et al., 2009); B: Per ascensum speleogenesis : model of the Lower Ardèche river (after Audra & Palmer, 2011)

Figure 6

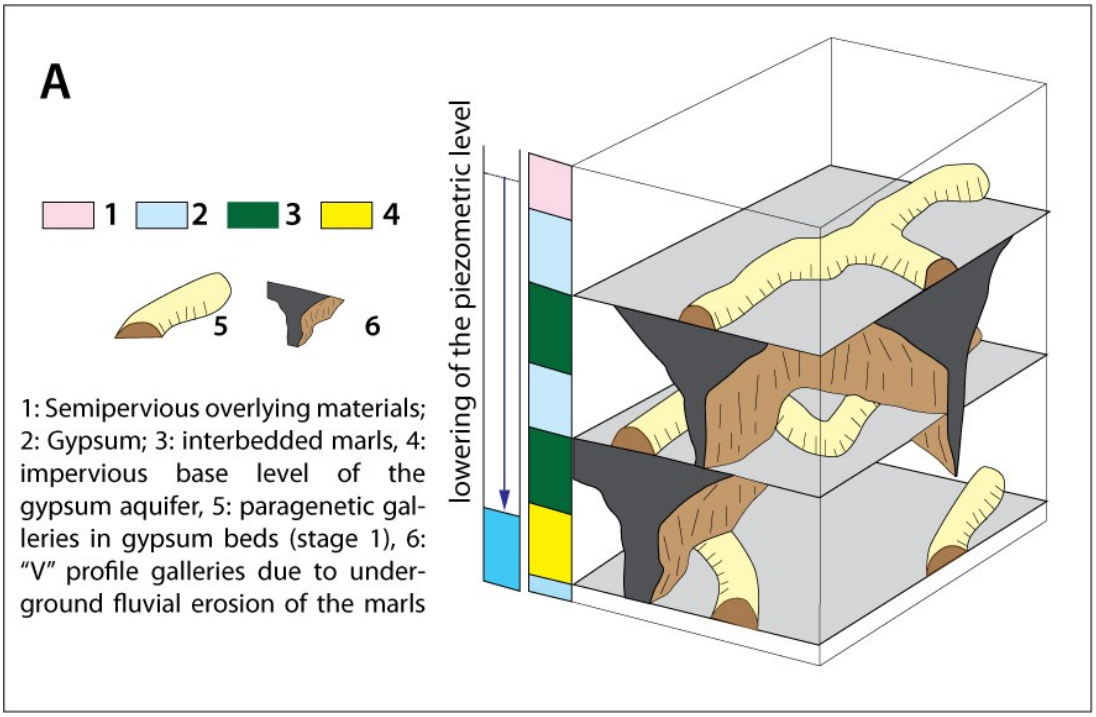
A
1
2
3
4
5
6
1: Semipervious overlying materials; 2: Gypsum; 3: interbedded marls, 4: impervious base level of the gypsum aquifer, 5: paragenetic galleries in gypsum beds (stage 1), 6: "V" profile galleries due to underground fluvial erosion of the marls
lowering of the piezometric level

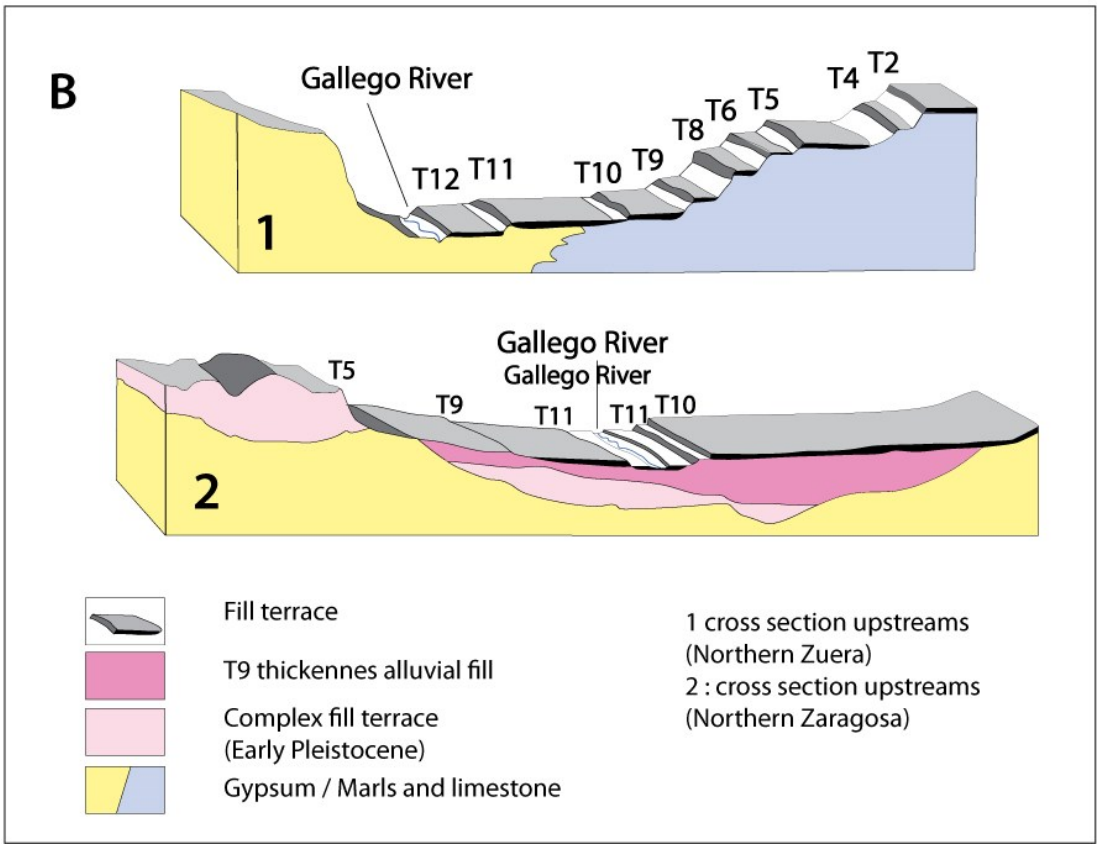
B
Gallego River
T12
T11
T10
T9
T8
T6
T5
T4
T2
1
Gallego River
Gallego River
T5
T9
T11
T11
T10
2
Fill terrace
T9 thickennes alluvial fill
Complex fill terrace
(Early Pleistocene)
Gypsum / Marls and limestone
1 cross section upstreams
(Northern Zuera)
2 : cross section upstreams
(Northern Zaragosa)

Figure 7

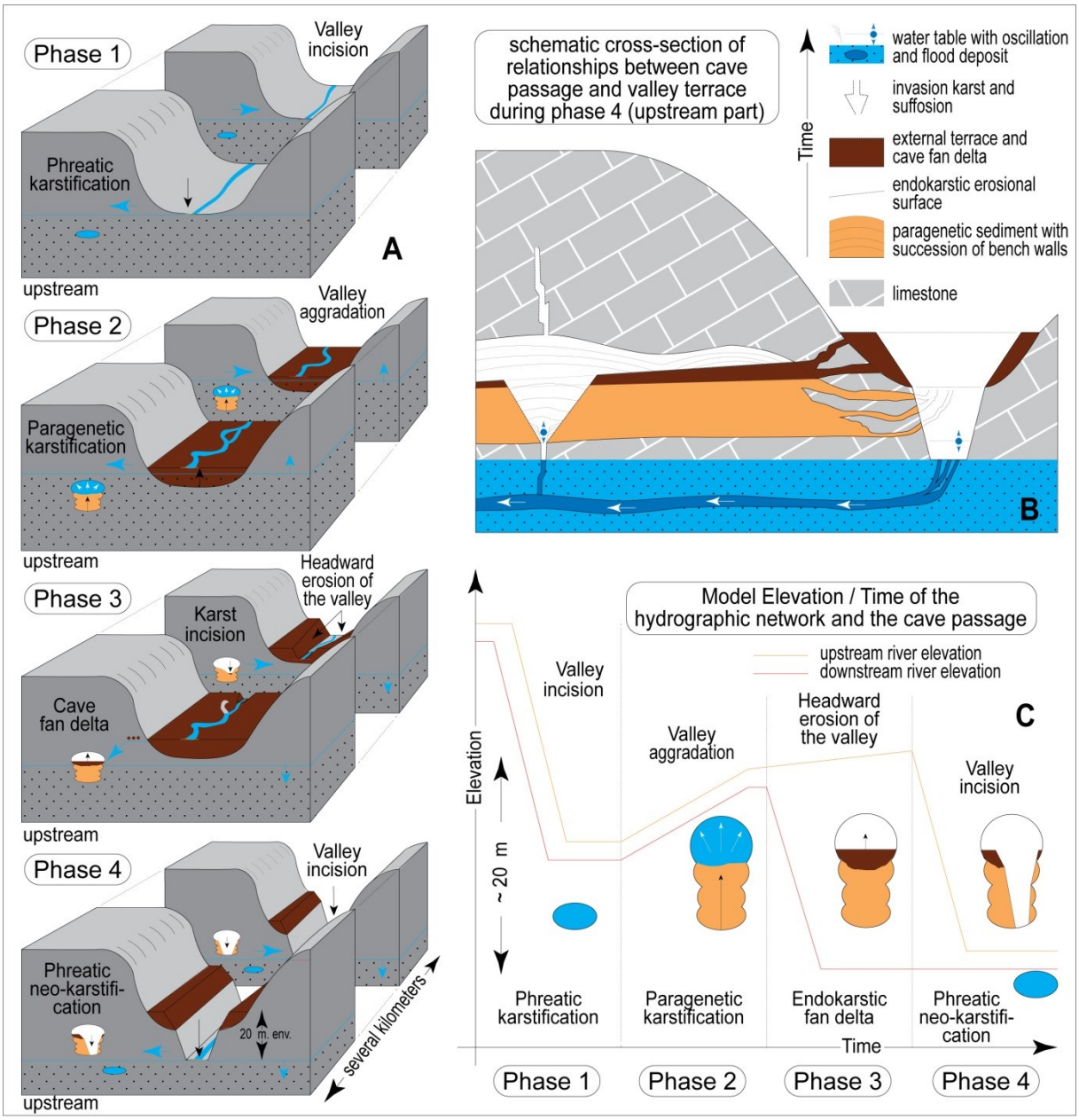

Figure 6

Figure 8:

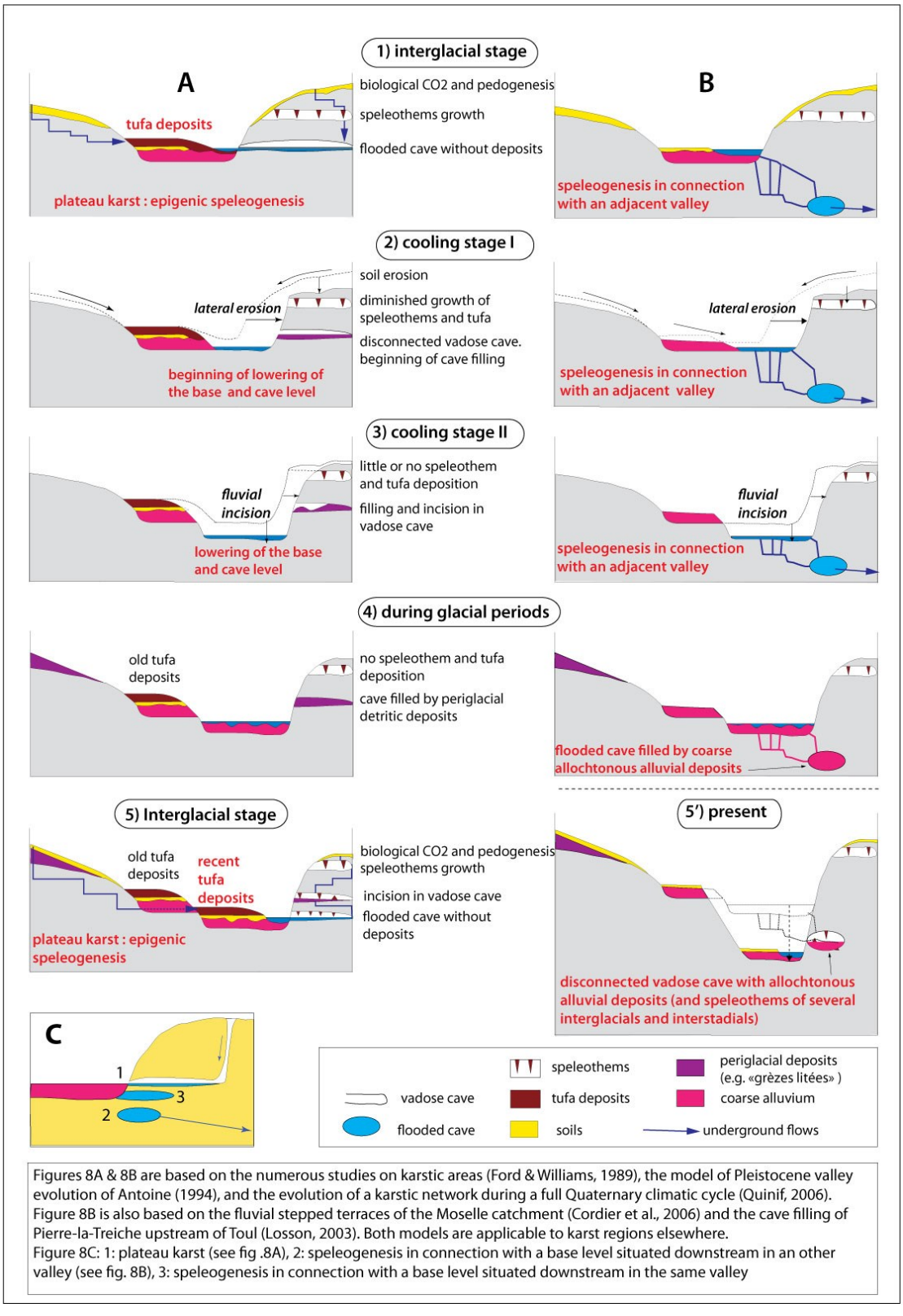

Figures 8A & 8B are based on the numerous studies on karstic areas (Ford & Williams, 1989), the model of Pleistocene valley evolution of Antoine (1994), and the evolution of a karstic network during a full Quaternary climatic cycle (Quinif, 2006). Figure 8B is also based on the fluvial stepped terraces of the Moselle catchment (Cordier et al., 2006) and the cave filling of Pierre-la-Treiche upstream of Toul (Losson, 2003). Both models are applicable to karst regions elsewhere.
Figure 8C: 1: plateau karst (see fig .8A), 2: speleogenesis in connection with a base level situated downstream in an other valley (see fig. 8B), 3: speleogenesis in connection with a base level situated downstream in the same valley

Figure 9:

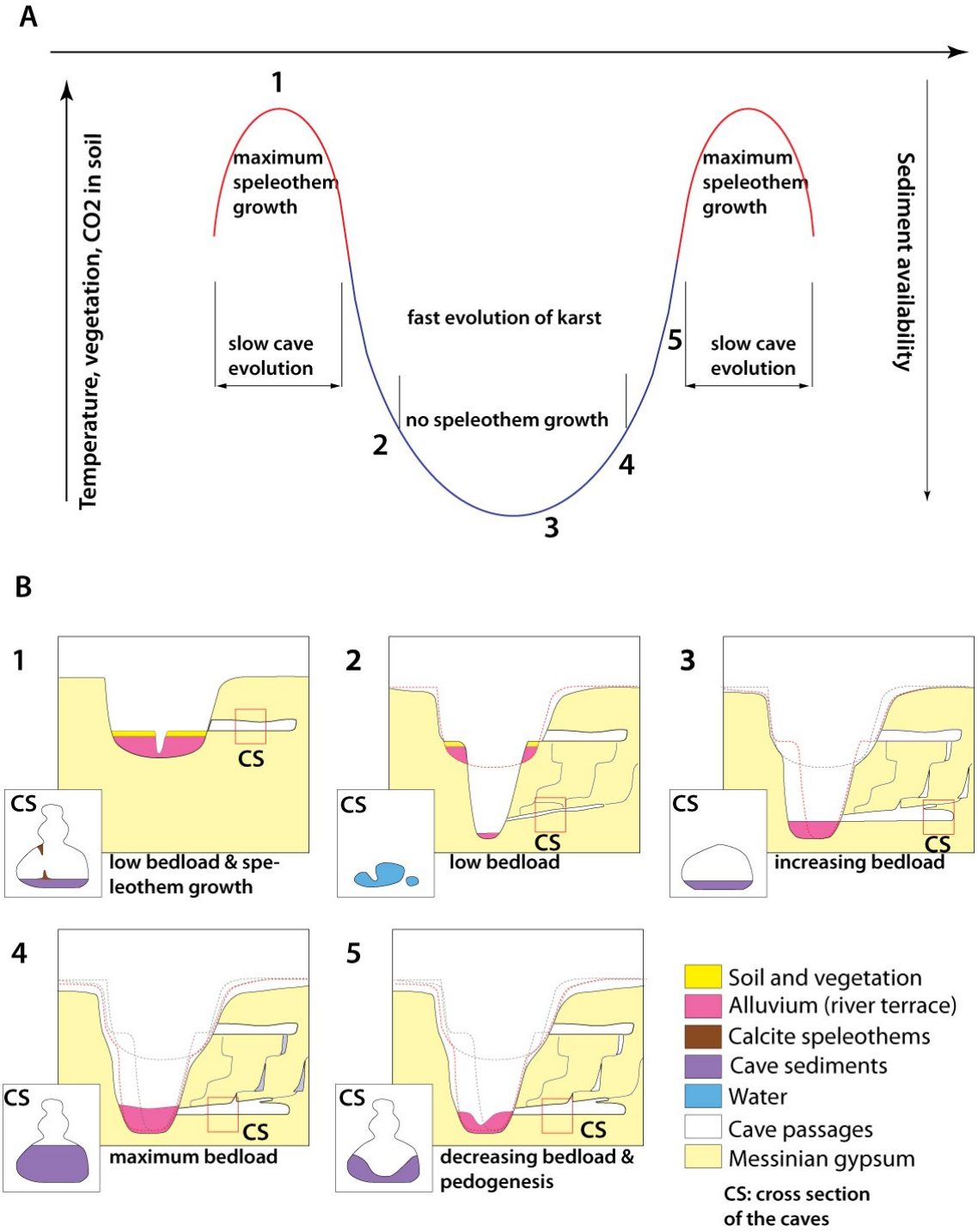
A
1
maximum speleothem growth
slow cave evolution
fast evolution of karst
no speleothem growth
2
3
4
5
maximum speleothem growth
slow cave evolution
Temperature, vegetation, CO2 in soil
Sediment availability
B
1
CS
low bedload & speleothem growth
2
CS
low bedload
3
CS
increasing bedload
4
CS
maximum bedload
5
CS
decreasing bedload & pedogenesis
Soil and vegetation
Alluvium (river terrace)
Calcite speleothems
Cave sediments
Water
Cave passages
Messinian gypsum
CS: cross section of the caves